Dalton Transactions

PAPER

View Article Online
View Journal

Cite this: DOI: 10.1039/c7dt02081c

Insertion reactions of small unsaturated molecules in the N–B bonds of boron guanidinates†

Alberto Ramos, *[a] Antonio Antiñolo, *[b] Fernando Carrillo-Hermosilla, [b] Rafael Fernández-Galán,[b] María del Pilar Montero-Rama,[b] Elena Villaseñor,[b] Antonio Rodríguez-Diéguez [c] and Daniel García-Vivó [d]

We report here 1,1- and 1,2-insertion reactions of small unsaturated molecules in the N–B bonds of two boron guanidinates, $(Me_2N)C(N^iPr)_2BCy_2$ (**1**) and $\{^iPr(H)N\}C(N^iPr)\{N(p\text{-}^tBu\text{-}C_6H_4)\}BCy_2$ (**2**), and two bis-boron guanidinates(2–), $\{^iPr(BCy_2)N\}C(N^iPr)\{N(p\text{-}^tBu\text{-}C_6H_4)\}BCy_2$ (**3**) and $\{^iPr(C_8H_{14}B)N\}C(N^iPr)\{N(p\text{-}Me\text{-}C_6H_4)\}BC_8H_{14}$ (**4**), the latter being prepared for the first time by double deprotonation of the corresponding guanidine with the 9-borabicyclo[3.3.1]nonane dimer, $(H\text{-}BC_8H_{14})_2$. Compounds **1–4** easily insert aromatic isonitriles, XylNC (Xyl = 2,6-Me_2-C_6H_3) and (*p*-MeO-C_6H_4)NC, to give the expected diazaboroles **5–12**, some of them being structurally characterised by X-ray diffraction. Interestingly, the BC_8H_{14} derivatives **11** and **12** are in a fast temperature-dependent equilibrium with the de-insertion products, whose thermodynamic parameters are reported here. A correlation between these equilibria and the puckered heterocyclic structure found in the solid state for **11**, and confirmed by DFT calculations, is also established. Reactions of the aforementioned guanidinates with CO are more sluggish or even precluded, and only one product, $\{^iPr(H)N\}C\{N(p\text{-}^tBu\text{-}C_6H_4)\}(N^iPr)(CO)BCy_2$ (**13**), could be isolated in moderate yields. The 1,2-insertions of benzaldehyde in compounds **1**, **2** and **4** are reversible reactions in all cases, and only one of the insertion products, $\{^iPr(H)N\}C\{N(p\text{-}^tBu\text{-}C_6H_4)\}(N^iPr)(PhHCO)BCy_2$ (**16a**), was isolated and diffractrometrically characterised. Likewise, CO_2 reversibly inserts into a N–B bond of **2** to give $\{^iPr(H)N\}C\{N(p\text{-}^tBu\text{-}C_6H_4)\}(N^iPr)(CO_2)BCy_2$ (**19**) with a conversion of *ca.* 9%. In all these equilibria, de-insertion is always favoured upon increasing the temperature.

Received 7th June 2017,
Accepted 10th July 2017

DOI: 10.1039/c7dt02081c

rsc.li/dalton

Introduction

In the last 20 years, the search for alternatives for cyclopentadienyl-based ligands in the fields of organometallic and coordination chemistry has led to the development of new N-donor ligands. Among them, guanidinato anions have played an important role.[1] These ligands display a planar 'CN_3' core and offer great electronic flexibility due to variable contributions of two main resonance forms: 1,3-diazaallyl (**I** and **II** in Scheme 1) and iminium-diamide (**III** in Scheme 1), depending on the electronic needs of the metal. Additionally, the steric and electronic properties of guanidinates can be easily tuned by the sensible choice of substituents. These outstanding features have contributed to the development of a rich coordination chemistry with most metals of the periodic table, in which the guanidinato ligand can display different coordination modes: κ^1-monodentate (not very common), κ^2-bidentate chelate or $\mu\text{–}\kappa^1\text{:}\kappa^1$-bridge (types **A**, **B** and **C** in Fig. 1).

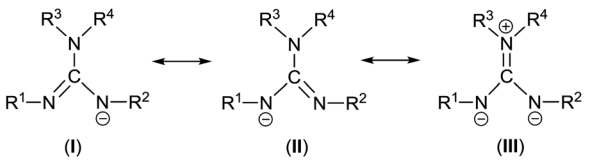

Scheme 1 Resonance structures for guanidinato ligands.

[a]*Departamento de Química Inorgánica, Orgánica y Bioquímica, Instituto Regional de Investigación Científica Aplicada, Universidad de Castilla-La Mancha, Campus Universitario, E-13071 Ciudad Real, Spain. E-mail: Alberto.Ramos@uclm.es*
[b]*Departamento de Química Inorgánica, Orgánica y Bioquímica-Centro de Innovación en Química Avanzada(ORFEO-CINQA), Universidad de Castilla-La Mancha, Campus Universitario, E-13071 Ciudad Real, Spain. E-mail: Antonio.Antinolo@uclm.es*
[c]*Departamento de Química Inorgánica, Facultad de Ciencias, Universidad de Granada, Avenida de la Fuente Nueva S/N, 18071 Granada, Spain*
[d]*Departamento de Química Orgánica e Inorgánica/IUQOEM, Universidad de Oviedo, E-33071 Oviedo, Spain*

†Electronic supplementary information (ESI) available: A CIF file containing crystallographic data for compounds **4**, **5**, **8a**, **10**, **11** and **16a**, plots, tables and NMR spectra used to determine thermodynamic parameters for isonitrile de-insertion reactions of compounds **11** and **12**, NMR spectra for new compounds, optimised structures of compounds **9–12** and an XYZ file containing Cartesian coordinates for all computed species. CCDC 1554010–1554015. For ESI and crystallographic data in CIF or other electronic format see DOI: 10.1039/c7dt02081c

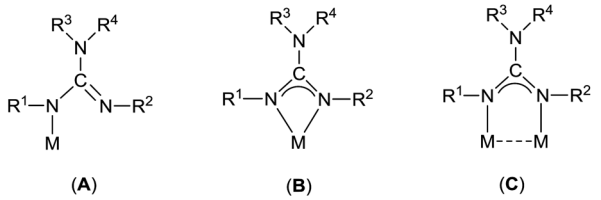

Fig. 1 Coordination modes for the guanidinato ligands.

Guanidinato compounds have also found applications in key technological areas such as homogeneous catalysis (olefin polymerisation, ring-opening polymerisation or amine guanylation) or materials science and nanotechnology (precursors for atomic layer deposition –ALD– or chemical vapour deposition –CVD– processes),[1b,d–g,i,k] and can be conveniently prepared by three main methods: (i) carbodiimide insertion in M–N bonds; (ii) guanidine deprotonation with metal alkyls or hydrides; (iii) salt metathesis between metal halides and alkali metal guanidinates.

In the last few years our group has focused on the synthesis of novel guanidinato compounds with early,[2] late[3] and s-block metals,[4] as well as the catalytic guanylation reaction.[2c,3a,4,5] As part of this study, we recently turned our attention to the relatively less explored chemistry of boron guanidinates.[6] Thus, in our previous report we prepared new symmetrical and asymmetrical dialkylboron guanidinates, as well as the first bis-boron guanidinate(2–), by salt metathesis from the corresponding lithium guanidinates and chloroboranes, employing commercially available or readily prepared reagents. Diffractometric studies revealed a chelate coordination (type **B**, Fig. 1) for the guanidinato ligands in these compounds. Their thermal stability was also tested revealing that, in some instances, carbodiimide de-insertion reactions took place even at room temperature in solution. These uncommon reactions (carbodiimide insertion reactions are usually favourable, being the most general method to prepare guanidinato compounds) were the subject of kinetic and thermodynamic studies, and a reaction mechanism was postulated, involving a switch of the coordination mode of the guanidinato, from κ^2-chelate to κ^1-monodentate, in the first step.

Since there is a limited number of examples of related boron(III) guanidinates in the literature and their chemistry remains largely unexplored,[7] we decided to focus now on the B–N insertion reactions of our dialkylboron guanidinates with small unsaturated molecules. In this sense, we were first inspired by the outstanding results recently published by Stephan and co-workers[8] on the FLP-type reactivity of related boron amidinates of the formula $[HC(NR)_2B(C_6F_5)_2]$ (R = ^{i}Pr, ^{t}Bu), towards small unsaturated molecules (Scheme 2) to give 1,1-insertions (with CO and isonitriles), 1,2-insertions (with CO_2, carbodiimides, benzaldehyde or acetonitrile) or heterolytic C–H cleavage (terminal alkynes). Previously, related work by Dorokhov and Mikhailov, who have extensively studied the reactivity of borylamidines, showed that *N*,*N*′-disubstituted boron amidinates of the formula $[PhC(NR)(NR')BR''_2]$ (R,R′ = alkyl, aryl; R″ = alkyl), with less electron-withdrawing groups on boron, were also able to react under mild conditions with isocyanates, aldehydes, aminoboranes (1,2-insertion reactions)[9] or isonitriles (1,1-insertion reactions)[10] but failed to react under harsher conditions with carbodiimides[11] or nitriles.[9]

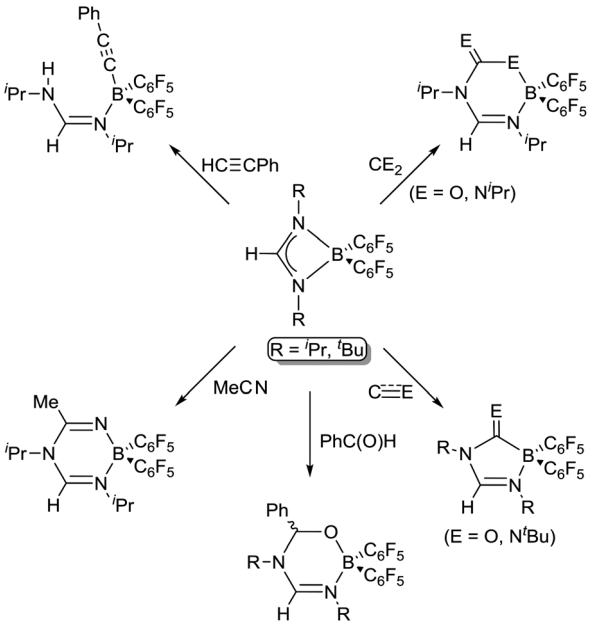

Scheme 2 FLP-type reactivity of boron amidinates $HC(NR)_2B(C_6F_5)_2$.[8]

With these precedents in mind, here we report the systematic reactivity study towards selected unsaturated molecules (isonitriles, CO, benzaldehyde and CO_2) of two dialkylboron guanidinates, a symmetrical and an asymmetrical one, $(Me_2N)C(N^iPr)_2BCy_2$ (**1**) and $\{^i$Pr(H)N$\}C(N^i$Pr$)\{N(p$-^{t}Bu-$C_6H_4)\}BCy_2$ (**2**),

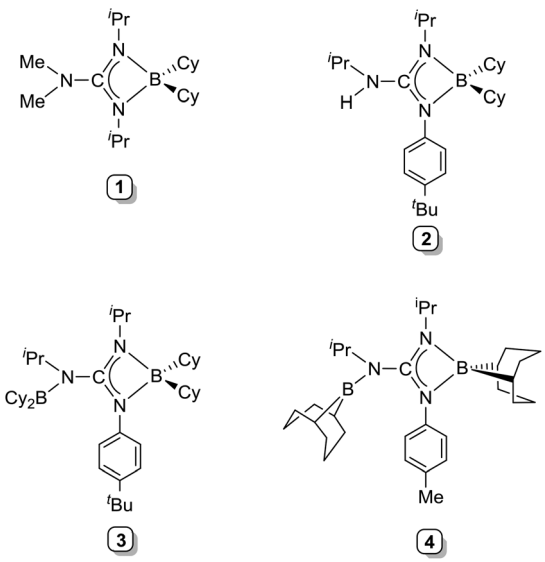

Fig. 2 Guanidinato compounds **1**–**4**.

and two bisboron guanidinates(2–), $\{^{i}Pr(BCy_2)N\}C(N^{i}Pr)\{N(p\text{-}^{t}Bu\text{-}C_6H_4)\}BCy_2$ (**3**) and $\{^{i}Pr(C_8H_{14}B)N\}C(N^{i}Pr)\{N(p\text{-}Me\text{-}C_6H_4)\}BC_8H_{14}$ (**4**) (Fig. 2), the latter being prepared for the first time by double deprotonation of the corresponding guanidine with the 9-borabicyclo[3.3.1]nonane dimer, $(H\text{-}BC_8H_{14})_2$. All these species were found to react with aromatic isonitriles, and some of them with CO to give 1,1-insertion products. Likewise, the addition of benzaldehyde and CO_2 led, in some instances, to 1,2-insertion products, in an equilibrium with the reagents.

Results and discussion

Solvent-dependent equilibrium for the isomers of compound 1

As mentioned above, four boron guanidinates with different steric and electronic properties were chosen to study their reactivity (Fig. 2). Although the synthesis and structural characterisation of compounds **1–3** were already described in our previous report,[6] we would like to note an important feature regarding compound **1**, which was unfortunately overlooked before. A careful analysis of different ^{1}H NMR spectra in C_6D_6 solution of this compound revealed the presence of small amounts (*ca.* 11%) of another species with inequivalent CH (^{i}Pr) groups, attributed to the monodentate isomer, **1-M**. The latter seems to be in a fast solvent-dependent equilibrium with the major species, the chelate isomer **1-C**, since upon changing the solvent to CD_2Cl_2, the relative amount of **1-M** increased slightly (Scheme 3). The presence of this monodentate isomer in solution, proposed as an intermediate in the carbodiimide de-insertion reaction,[6] is not so surprising even when this is the least abundant coordination mode for such ligands in the literature.[1c] In fact, Dorokhov and Mikhailov already detected this type of solvent-dependent equilibrium in dialkylboron amidinates of the formula $[PhC(NMe)_2BR_2]$ (R = Pr, Bu).[9] Moreover, a monodentate coordination was also postulated for the first boron guanidinates reported in the literature by Lappert and co-workers, $[(Et_2N)C\{N(p\text{-}tol)_2\}BXY]$ (XY = Ph_2; Ph, SBu; Ph, NEt_2; $o\text{-}O_2C_6H_4$), on the basis of IR spectra,[7a] as well as for the boron amidinate $[HC(NCy)_2BC_8H_{14}]$, on the basis of ^{11}B NMR,[12] overall indicating that the monodentate coordination of amidinato/guanidinato ligands to boron centres is not that unusual. Finally, it should be noted that the detection of a monodentate guanidinate isomer for **1** is rather important for the insertion reactions we present herein from a mechanistic point of view, since Stephan postulated an open-chain form of the strained chelate as the active species for the FLP-type reactivity of their boron amidinates, which they failed to detect in solution even after increasing the temperature up to 80 °C.[8]

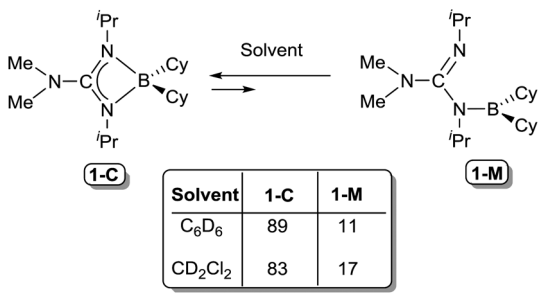

Solvent	1-C	1-M
C_6D_6	89	11
CD_2Cl_2	83	17

Scheme 3 Solvent-dependent equilibrium for compound **1**.

Synthesis and structural characterisation of compound 4

As mentioned in Introduction, compounds **1–3** were prepared from a metathetical synthetic route, therefore generating lithium chloride as an undesired side product. In order to test an alternative, more atom-efficient route to prepare boron guanidinates we tried the direct deprotonation of a guanidine with a commercial secondary borane. Pleasingly, double deprotonation of $(p\text{-}Me\text{-}C_6H_4N)C(NH^{i}Pr)_2$ with one equivalent of the dimer $(H\text{-}BC_8H_{14})_2$ proceeded smoothly in toluene under mild conditions (room temperature, 4 h) to give the novel bisboron guanidinate(2–) **4** in good yields.

The molecular structure of compound **4** was determined by a diffractometric analysis (Fig. 3, Table 1). This compound crystallised in the triclinic $P\bar{1}$ space group. The main structural features of this compound are reminiscent of those found for compound **3**, previously described.[6] Thus, two N atoms (N1

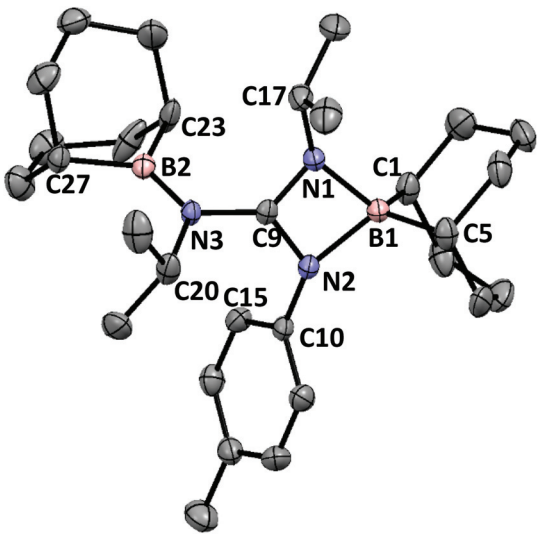

Fig. 3 Molecular structure of compound **4**: H atoms are omitted for clarity and ORTEP ellipsoids are plotted at the 50% probability level.

Table 1 Selected bond lengths (Å) and angles (°) for compound **4**

B1–N1	1.631(2)	C1–B1–C5	108.5(1)
B1–N2	1.637(2)	N1–B1–N2	79.4(1)
C9–N1	1.318(2)	N1–C9–N2	103.7(1)
C9–N2	1.335(2)	N1–C9–N3	128.5(1)
C9–N3	1.404(2)	N2–C9–N3	127.8(1)
N3–B2	1.416(2)	C9–N3–B2	120.8(1)
N1–C17	1.464(2)	C20–N3–B2	126.1(1)
N2–C10	1.421(2)	C9–N3–C20	113.1(1)
N3–C20	1.502(2)	C15–C10–N2–C9	49.6(2)

and N2) of the guanidinato ligand in compound **4** are chelating one of the boron centres (B1), defining an almost planar four-membered CN_2B heterocycle as denoted by the low torsion angle between the CN_2 and N_2B planes of 5.5°. Conversely, the exocyclic N3 presents a κ^1-monodentate coordination mode to the other tricoordinate B atom. The C–N distances within the guanidinato core are intermediate between the typical single and double C–N bonds, as expected due to the contribution of the different resonance forms (Scheme 1). However, C9–N3 is somewhat longer than the other two, 1.40 Å *vs.* 1.33 and 1.32 Å, which fits well with a much lower contribution of the "iminium diamide" resonance form, also observed for compound **3**. As in the latter case, this is consistent with the involvement of the lone pair on N3 on a π interaction with B2, confirmed by the B2–N3 distance of 1.416(2) Å, which falls in the range found for B–N distances in aminoboranes with significant π (B=N) bonding (1.41–1.45 Å).[13] Moreover, the sum of angles at B2 and N3 is practically 360°, so that an sp^2 hybridisation can be safely assigned to both atoms, which further confirms our hypothesis. Focusing on the exocyclic borylamine group, a strongly staggered conformation with respect to the heterocycle can be clearly detected, with a C20–N3–B2/N1–C9–N2 torsion angle of 62.5°, somewhat smaller than that measured for compound **3** of 77.9°. In any case, this arrangement also hampers the electron overlapping with the rest of the guanidinato ligand, which, alongside the elongated C9–N3 distance, agrees well with an almost negligible contribution of the "iminium diimide" resonance structure. There is some degree of pyramidalisation on the N atoms chelating B1, not observed for compound **3**. This is denoted by the sum of angles at N1 and N2, 355.8 and 353.1° and the fact that the N–^{i}Pr and N–Ar groups are pointing out of the heterocycle plane on opposite directions, with average angles of 21.8 and 24.1°, respectively. This is probably due to the steric congestion on the BN_2C plane induced by the cyclic C_8H_{14} fragment bound to B1, also causing a staggered conformation of the aryl ring with respect to the latter plane, with a C15–C10–N2–C9 torsion of 49.6(2)° compared to 22.2(4)° measured for the same torsion angle in **3**.[6]

The solution NMR characterisation of **4** is in good agreement with the solid state structure of the compound (see Table 2). The absence of symmetry elements in the molecule is evident in the multinuclear NMR spectra recorded for **4**. For example, two couples of diastereotopic methyls attributed to the N–^{i}Pr groups give rise to four different doublets, at 1.32 and 1.23 ppm, and 0.95 and 0.82 ppm, respectively. Each pair is coupled to a methyne proton, giving rise to the corresponding septets at 3.83 and 3.54 ppm. The lack of symmetry of **4** is also evident in the $^{13}C\{^1H\}$ NMR, which displays four and two signals, respectively, for the CH_3 and CH groups of these N–^{i}Pr moieties. Additionally, up to 12 different signals between 35 and 22 ppm could be assigned to both BC_8H_{14} groups, instead of the 16 expected, probably due to the accidental degeneracy of some of the signals. The ^{11}B NMR spectrum shows two broad signals, *ca.* 53 and 13 ppm, respectively, attributed to the tri- and tetracoordinate boron, and comparable to those found for the isostructural compound **3**.[6]

1,1-Insertion reactions of compounds 1–4 with isonitriles and CO

The reactivity of the guanidinato compounds **1–4** was tested towards isonitriles in the first place. Interestingly, they all failed to react with ^{t}BuNC even at 80 °C, but instead proved to be quite reactive towards less sterically-demanding aromatic isonitriles, such as XylNC (Xyl = 2,6-Me_2-C_6H_3) or (*p*-MeO-C_6H_4)NC even at room temperature to give the

Table 2 Selected IR and NMR data for new compounds

		δ_H (ppm) [J_{HH} in Hz][a]			
Compound	ν (cm^{-1})	C*H*-^{i}Pr	N*H*	C*H*$_3$-^{i}Pr	δ_B[a] (ppm)
4	—	3.83 [6.7], 3.54 [6.9]	—	1.32 [6.7], 1.23 [6.7], 0.95 [6.9], 0.82 [6.9]	53.2, 12.6
5	1638 (s, C=N)	3.57 [6.8], 3.32 [6.8]	—	1.60 [6.8], 1.14 [6.8]	1.6
6	1638 (s, C=N)	3.59 [6.8], 3.30 [6.8]	—	1.60 [6.8], 1.12 [6.8]	1.6
7a	3453 (w, N–H), 1649 (s, C=N)	5.25 [br], 2.97 [9.2, 6.3]	3.86 [9.2]	1.22 [br], 0.60 [6.3]	0.6
7b	—	3.82 [7.2], 2.74 [8.9, 6.4]	3.55 [8.9]	1.14 [7.2], 0.52 [6.4]	—
8a	3346 (w, N–H), 1638 (s, C=N)	5.20 [br], 2.96 [9.4, 6.3]	3.79 [9.4]	1.33 [6.8], 0.61 [6.4]	0.7
8b	—	3.78 [7.2], 2.82 [9.2, 6.4]	3.69 [9.2]	1.12 [7.2], 0.61 [6.4]	—
9	1634 (m, C=N)	4.10 [6.7], 3.40 [br]	—	1.79 [6.7], 1.75 [6.7], 1.2 [vbr], 0.9 [vbr]	49.5, 1.5
10	1652 (m, C=N)	4.07 [6.7], 3.46 [6.9, 6.6]	—	1.78 [6.7], 1.77 [6.7], 1.25 [6.9], 0.92 [6.6]	51, −2
11	1648 (m, C=N)	4.15 [6.7], 2.97 [6.7]	—	1.79 [6.7], 1.72 [6.7], 0.95 [6.7], 0.41 [6.7]	56.3, 2.5
12	1633 (m, C=N)	4.10 [6.7], 2.97 [6.7]		1.78 [6.7], 1.71 [6.7], 0.98 [6.7], 0.35 [6.7]	52.5, 2.7
13	3294 (m, N–H) 1674 (s, C=O)	4.59 [br], 3.06 [9.3, 6.4]	4.05 [9.3]	1.19 [≈7], 0.61 [6.4]	2.1
14	—	3.74 [6.7], 2.93 [6.7]	—	1.60 [6.7], 1.53 [6.7], 0.94 [6.7], 0.40 [6.7]	—
15	—	3.98 [≈7], 3.35 [≈7]	—	1.19 [≈7], 1.10 [≈7], 0.94 [≈7], 0.86 [≈7]	—
16a	3389 (w, N–H)	3.87 [6.8], 3.52 [9.4, 6.4][b]	3.63 [9.4][b]	1.27 [≈7], 1.10 [6.4], 1.05 [6.8], 0.94 [6.4][b]	8.0[b]
16b	—	4.07 [≈7], 3.14	3.89 [≈7]	—	—
17	—	4.27 [6.9], 3.22 [6.7]	—	1.31 [6.9], 0.92 [6.7], 0.48 [6.9], 0.40 [6.7]	—
18	—	3.76 [≈7], 3.20	3.85 [8.7]	1.22 [≈7], 0.78 [≈7], 0.59 [≈7], 0.58 [≈7]	—
19	—	3.88 [6.7], 2.99 [9.2, 6.3]	3.44 [9.2]	1.56 [6.7], 0.47 [6.3]	—

[a] In C_6D_6 at 298 K at 400 or 500 MHz (^1H), or 128 MHz (^{11}B) unless otherwise stated. [b] In CD_2Cl_2.

expected 1,1-insertion products. Thus, compound **1** reacted in *ca.* 2 h with the latter isonitriles to give compounds $(Me_2N)C(N^iPr)_2(CNAr)BCy_2$ [Ar = Xyl (**5**), *p*-MeO-C_6H_4 (**6**)], which were isolated as microcrystalline solids in good yields (Fig. 4). The reaction of the asymmetrical guanidinato compound **2** towards the same isonitriles took also place at room temperature in *ca.* 2 h. However, in this case, two regioisomers were possible, depending on which N–B bond the insertion took place. Monitoring the reactions by ^{1}H NMR in C_6D_6 (Fig. S13 and S15, ESI†) revealed that, indeed, a mixture of the two possible regioisomers was obtained with both isonitriles, $\{^iPr(H)N\}C\{N(p\text{-}^tBu\text{-}C_6H_4)\}(N^iPr)(CNAr)BCy_2$ [Ar = Xyl (**7a**), *p*-MeO-C_6H_4 (**8a**)], and $\{^iPr(H)N\}C(N^iPr)\{N(p\text{-}^tBu\text{-}C_6H_4)\}(CNAr)BCy_2$ [Ar = Xyl (**7b**), *p*-MeO-C_6H_4 (**8b**)] (Fig. 4). In both instances, the major isomer is the one in which the insertion takes place in the ^{i}PrN–B bond, with ratios **7a** : **7b** and **8a** : **8b** of 6 : 1 and 3 : 1, respectively. It is worth mentioning as well that these isomers do not seem to be in a temperature-dependent equilibrium in solution, since there are no changes in their relative ratio upon warming the solutions up to 60 °C. Of the latter isomer mixtures, only the major species, **7a** and **8a**, could be isolated as crystalline solids, the others being only detected by some characteristic signals in the ^{1}H NMR spectra (see Table 2). Interestingly, the reaction of bisboron guanidinate(2–) **3** towards these isonitriles was slower, probably owing to the higher steric hindrance and reduced basicity of the chelate N atoms induced by the exocyclic $N(^iPr)BCy_2$ group, but much more regioselective, and insertions only took place in the endocyclic ^{i}PrN–B bond to give compounds $\{^iPr(BCy_2)N\}C\{N(p\text{-}^tBu\text{-}C_6H_4)\}(N^iPr)(CNAr)BCy_2$ [Ar = Xyl (**9**), *p*-MeO-C_6H_4 (**10**)] almost quantitatively after at least 2 days at room temperature. Similar regioselectivity was achieved in the reactions of **4** with isonitriles, which, upon mixing, led to the insertion products $\{^iPr(BC_8H_{14})N\}C\{N(p\text{-Me-}C_6H_4)\}(N^iPr)(CNAr)BC_8H_{14}$ [Ar = Xyl (**11**), *p*-MeO-C_6H_4 (**12**)] (Fig. 4). These compounds turned out to be in a temperature-dependent equilibrium with the reagents, shifted towards the insertion products at room temperature, which will be discussed in more detail later.

The reactivity of compounds **1–4** was also tested towards CO. In general terms, these reactions turned out to be more sluggish than their counterparts with isonitriles, especially for the BCy_2 derivatives. This observation goes in line with that reported by Stephan and co-workers for the more active boron amidinates $[HC(NR)_2B(C_6F_5)_2]$ (R = ^{i}Pr, ^{t}Bu).[8] Thus, we were only able to isolate one carbonylation product in moderate yields, this being $\{^iPr(H)N\}C\{N(p\text{-}^tBu\text{-}C_6H_4)\}(N^iPr)(CO)BCy_2$ (**13**), obtained after exposing compound **2** to an atmosphere of CO (*ca.* 4 atm) at 40 °C for 3 days (Scheme 4). Interestingly, CO insertion was not observed for compound **1** at room temperature, and instead the expected carbodiimide de-insertion reaction took place progressively, accelerated upon increasing the temperature (50 °C).[6] As for compound **3**, when subjected to similar reaction conditions (3 days, 50 °C, 4 atm), the major compound in solution was still unreacted **3**, and only small amounts of other species were detected by NMR. Unfortunately, signals attributed to the expected insertion product could not be unambiguously assigned. However, one of the species detected was compound **13**, suggesting that, to a lesser extent, carbonylation also took place, but the product obtained must be very reactive under these conditions to give compound **13** after partial hydrolysis of the exocyclic N–B bond. Remarkably, as opposed to compounds **1–3**, compound **4** reacted immediately upon exposure to CO (1 atm) to give the insertion product $\{^iPr(BC_8H_{14})N\}C\{N(p\text{-Me-}C_6H_4)\}(N^iPr)(CO)BC_8H_{14}$ (**14**), which is in equilibrium with the de-insertion compounds, **4** and CO, clearly shifted towards the reagents at

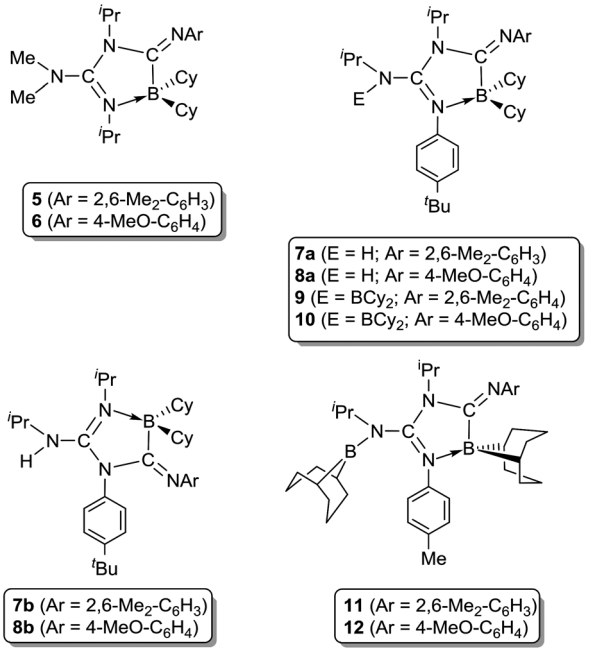

Fig. 4 Compounds **5–12**.

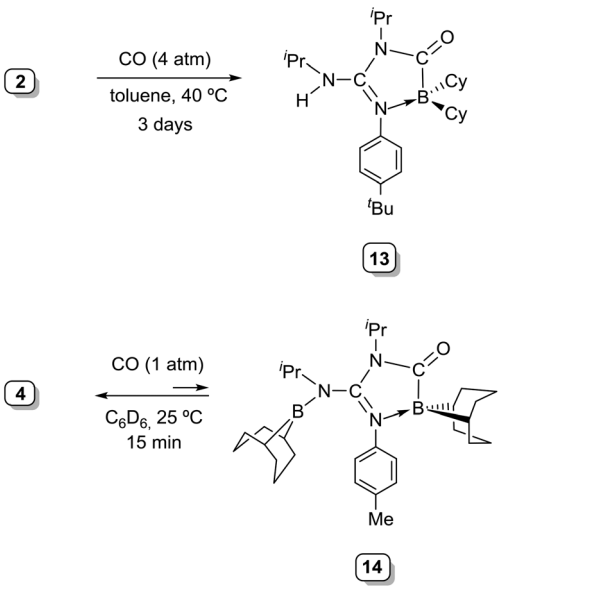

Scheme 4 Reactions of compounds **2** and **4** towards CO.

room temperature (ratio **4 : 14** *ca.* 9 : 1). Structural nuances between the borabicyclic BC_8H_{14} and the BCy_2 seem to be behind the difference in reactivity between compounds **1–3** *vs.* compound **4** towards isonitriles and CO, as will be addressed in the next section.

At this stage, some mechanistic considerations should be briefly commented regarding the 1,1-insertion reactions of isonitriles and CO in boron guanidinates **1–4**. We assume that, in a first stage, an open-chain intermediate (detected in the case of **1-M**) is required in order to react with the incoming unsaturated molecule. This was also assumed by Stephan and co-workers[8] for FLP-type reactions of boron amidinates and later corroborated by DFT calculations.[14] After this step, two pathways are possible, one involving a concerted insertion mechanism[14] and the other a two-step process involving the formation of the EC–borane adduct (E = O, NR) and subsequent nucleophilic attack by the N atom to the C atom of the isonitrile or CO to give the five-membered heterocycle. Although we have not detected an intermediate suggesting the formation of such an adduct, Erker and co-workers did find them in the reactions of intramolecular P/B FLPs of the formula $Ph_2PC(p\text{-Tol}){=}CRB(C_6F_5)_2$ (R = C_6F_5, Me) with CN^tBu, which turned out to be in temperature-dependent equilibria with the 1,1-insertion products and the reagents.[15] As for the regioselectivity of the 1,1-insertion reactions herein studied with the asymmetrical guanidinates **2–4**, as mentioned before, in all cases the major (or only) product detected is the one resulting from the insertion in the endocyclic ^{i}PrN–B bond. This could be explained in terms of the enhanced donor ability of the more basic N centre [N(^{i}Pr) > N(Ar)]. Interestingly, compound **1**, for which the open chain isomer was detected, **1-M**, was not the most reactive species in these 1,1-insertion reactions, which suggests that the presence of an open-chain isomer in solution is a not sufficient condition for this type of reactivity, and other electronic and steric factors may be influential as well (*e.g.*, sufficient degree of basicity/acidity at the N/B centres, or less steric hindrance around the chelating N centres and the tetracoordinate boron).

Structural characterisation of 1,1-insertion products 5–14

The solid-state structures of the isonitrile insertion products **5**, **8a**, **10** and **11** were determined by X-ray diffraction analyses (Fig. 5, Table 3). These compounds crystallised in the monoclinic space groups $P2_1/c$ (**5**) and $P2_1/n$ (**11**), and the triclinic space group $P\bar{1}$ (**8a** and **10**). As can be seen, they all share many common features and will be therefore discussed together. However, some differences are also evident between the molecule of **11** and the other three compounds. Thus, despite being all built around five-membered heterocycles (diazaboroles), compounds **5**, **8a** and **10** display a roughly planar arrangement as indicated by the sum of internal angles of *ca.* 540°, whereas this ring is clearly puckered for **11** (530.7°). Indeed, the latter compound displays a half chair configuration in which the C2 and B1 atoms are located at different sides of the plane defined by the CN_3 core of the guanidine, as denoted by the N2–C1–N1/B1–C2–N2 torsion angle of 25.7°. In contrast, compounds **5**, **8a**, and **10** only show slight deviations from planarity (N2–C1–N1/B1–C2–N2 < 8°). The half-chair conformation of **11** could be explained on steric grounds, as the cyclic C_8H_{14} group on B1 seems to induce higher steric pressure on the neighbouring bulky groups of the diazaborazole ring [N(*p*-tolyl) and C═NXyl], as opposed to two Cy

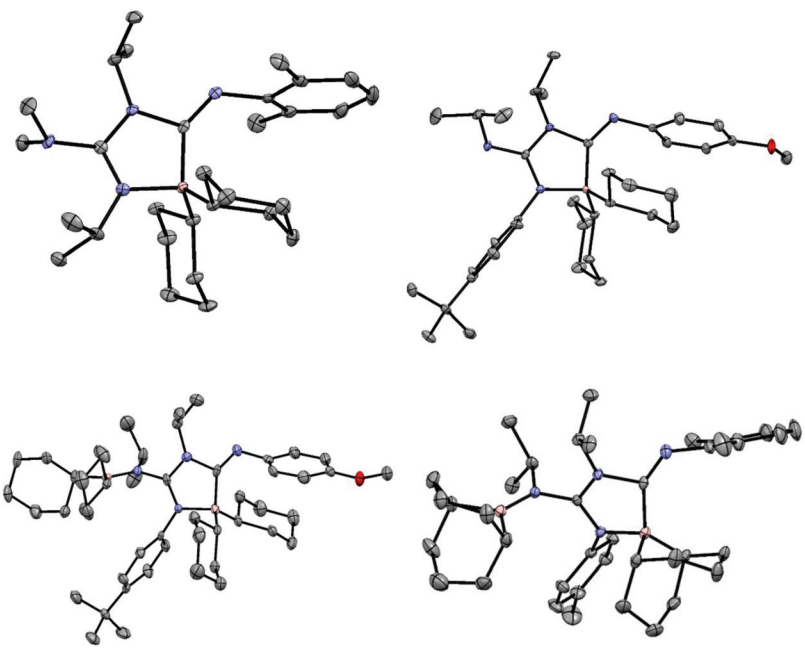

Fig. 5 Molecular structures of compounds **5** (top left), **8a** (top right), **10** (bottom left) and **11** (bottom right): H atoms are omitted for clarity and ORTEP ellipsoids are plotted at the 50% probability level. Colour code: C, grey; B, pink; N, blue; O, red.

Table 3 Selected bond lengths (Å) and angles (°) for compounds **5**, **8a**, **10** and **11**[a]

Compound	5	8a	10	11
B1–N1	1.618(4)	1.629(2)	1.645(6)	1.624(2)
N1–C1	1.294(3)	1.313(2)	1.310(6)	1.317(2)
C1–N2	1.368(4)	1.358(2)	1.362(5)	1.350(2)
C1–N3	1.403(3)	1.372(2)	1.419(6)	1.414(1)
N2–C2	1.432(3)	1.436(2)	1.449(6)	1.463(2)
C2–B1	1.658(4)	1.654(2)	1.637(7)	1.642(2)
C2–N4	1.281(4)	1.279(2)	1.282(5)	1.275(2)
N4–C6	1.409(3)	1.416(2)	1.421(6)	1.410(2)
N3–B2	—	—	1.432(5)	1.417(2)
N1–B1–C2	96.0(2)	94.7(1)	94.6(3)	94.9(1)
B1–C2–N2	106.0(2)	107.8(1)	108.0(4)	102.5(1)
C2–N2–C1	111.5(2)	110.7(1)	111.2(4)	110.3(1)
N2–C1–N1	114.5(2)	114.3(1)	113.5(4)	113.5(1)
N2–C1–N3	123.3(2)	121.5(1)	121.5(4)	122.2(1)
N3–C1–N1	122.2(2)	124.1(1)	124.9(4)	124.2(1)
C1–N1–B2	111.5(2)	112.1(1)	112.6(3)	109.5(1)
N2–C1–N1/B1–C2–N2[b]	5.0	7.5	3.6	25.7

[a] Values according to the labelling shown in the picture below. [b] Torsion between the planes.

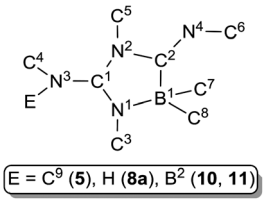

E = C^9 (**5**), H (**8a**), B^2 (**10**, **11**)

groups, which can be arranged perpendicularly at both sides of the heterocyclic plane reducing the steric impact on the closer groups. Thus, in order to minimise the steric congestion in **11**, the BC_8H_{14} is pointing out of the N1–C1–N2 plane, whereas the *p*-tolyl and C═NXyl groups are projecting outwards on the opposite side of the plane.

In order to rule out the possibility of packing effects accounting for the puckered ring found for compound **11**, the structures of compounds **9–12** were optimised using Density Functional Theory (DFT) methods (Fig. S28 in the ESI†). Overall, the structural parameters of all these compounds are essentially identical to those experimentally measured for **10** and **11**, including the presence of significantly puckered five-membered rings in the two BC_8H_{14} derivatives, **11** and **12**, and five-membered planar rings for the two BCy_2 derivatives computed, **9** and **10**. This implies that the puckering in the BC_8H_{14} derivatives has a genuinely steric or electronic origin. Moreover, a constrained optimisation of the geometry of compound **11** to retain a planar central ring akin to that observed for the BCy_2 derivatives (Fig. S29 in the ESI†) yielded a structure located 7.3 kcal mol^{-1} above the corresponding puckered (not-restrained) structure. Interestingly, the cyclic B atom in the forcedly planar structure of **11** displays quite asymmetric bond distances (B–C = 1.686 Å and B–N = 1.619 Å), this further confirming the idea that an unbearable steric pressure is exerted by the BC_8H_{14} group on planar dispositions. Examples of structurally related species in the literature, such as Stephan's diazaboroles $HC(N^iPr)_2(CE)B(C_6F_5)_2$ (E = O, N^tBu)[8] or Warren's oxazaborole $HC(NAr')(O)(NXyl)B(C_6F_5)_2$ (Ar′ = 4-^{t}Bu-2,6-Ph_2-C_6H_2)[16] displayed planar five-membered rings similar to **5**, **8a**, and **10**, which makes compounds **11** and **12** rather unique examples.

The other structural parameters found in the solid state for the four compounds are very similar. For example, the two new bonds formed upon insertion of the isonitrile in one of the N–B bonds, *i.e.*, N2–C2 and C2–B2, with distances *ca.* 1.43–1.46 Å and 1.64–1.66 Å, respectively, fall in the ranges expected for single N–C and C–B bonds. The inserted isonitrile has now become an exocyclic imine (*E* isomer in all cases), as denoted by the C2–N6 distances, *ca.* 1.28 Å, consistent with the formulation of double C═N bonds. There is less π delocalisation along the C–N bonds of the parent guanidinato moiety, with distances following this sequence: C1–N1 (1.29–1.32 Å) < C1–N2 (1.35–1.37 Å) < C1–N3 (1.37–1.42 Å), suggesting higher localisation of the π electrons on the C1–N1 bond (*i.e.*, more double C═N bond character), and almost negligible for the exocyclic C1–N3 (*i.e.*, essentially a single C–N bond), especially so for the bisboron derivatives **10** and **11** (C1–N3 distances *ca.* 1.42 Å). This is in good agreement with the almost perpendicular arrangement of the substituents at the exocyclic N3 within these compounds, (B2–N3–C4/N1–C1–N2 torsion angles of 75.2 and 87.7° for **10** and **11**, respectively). Moreover, the sum of angles about N3 and B2 atoms in these compounds (*ca.* 360°), as well as the N3–B2 distances, are consistent with a strong π N═B bonding, like in the parent guanidinates **3** and **4**. Finally, in all four structures, the planar arrangement of the CN_3 core of the guanidinato moiety is evidenced by the trigonal planar arrangement around the central C1 atom (sum of angles *ca.* 360°), indicative of an sp^2 hybridisation.

Compounds **5–14** were also characterised by multinuclear NMR in solution and by ATR-IR in the solid state (Table 2), except for those species that could not be isolated, which were only detected by ^{1}H NMR (**7b**, **8b** and **14**). In the first place, the IR spectra of compounds **5–12** display a medium-to-strong band in the frequency range expected for the stretch of double C═N bonds (1634–1652 cm^{-1}), attributed to the imine functionality formed upon insertion of the isonitrile and comparable to those observed for related diazaborazoles of the formula $[RC(NR')_2(CNPh)BR''_2]$ (R, R′ = alkyl, aryl; R″ = alkyl).[10] As expected, compound **13** exhibits a C–O stretch band at slightly higher frequencies, 1674 cm^{-1}, attributed to the double C═O bond, although >40 cm^{-1} below those found for related diazaborazoles with the more electron withdrawing C_6F_5 groups on boron.[8,17] Additionally, the N–H stretch was also assigned to a weak band in the range 3294–3453 cm^{-1} in the IR spectra of compounds **7a**, **8a**, and **13**.

The NMR spectroscopic data for these compounds are, overall, in good agreement with the solid-state structures of the diazaborazoles commented before. For example, the ^{11}B NMR spectra exhibit either one or two signals for the tetra- and tricoordinate boron atoms (the latter, of course, only for bisboron derivatives **9–12**), at the expected chemical shifts, *ca.* 0 and 50 ppm, respectively. We should note here that tetracoor-

dinate borons resonate some 10 ppm upfield from those of the parent boron guanidinates **1–4**, perhaps due to the replacement of one B–N bond by a new B–C bond, an effect also observed in Stephan's amidinates.[18] ^{1}H and ^{13}C{^{1}H} NMR spectra for the bisboron derivatives, **9–12** and **14**, are consistent with the low symmetry (C_1) observed in the previous diffractometric studies. Thus, each ^{i}Pr group gives rise to two signals for the diastereotopic CH_3 moieties in both spectra. Likewise, up to sixteen different signals could be assigned to two different BC_8H_{14} groups in the carbon-13 spectra for compounds **11** and **12**, whereas four inequivalent Cy groups generated more complex spectra with some broad overlapping signals for compounds **9** and **10**, also indicating some dynamic behaviour as will be commented below.

In contrast, compounds **5–8**, and **13** show a higher apparent symmetry, most likely due to fast rotation in the NMR timescale of the exocyclic amino groups (NMe_2 or $NH^{i}Pr$) in solution at room temperature. This would generate a false symmetry plane containing the diazaborole ring, thus making the Me groups within each ^{i}Pr equivalent. Indeed, each ^{i}Pr group generates only one signal due to the CH_3 moieties in their ^{1}H and ^{13}C NMR spectra. Moreover, the now equivalent Cy groups originate up to six signals (sometimes less due to accidental degeneracy or overlapping) in the carbon-13 spectra for compounds **5**, **6**, **7a**, **8a** and **13**. Other significant signals in the ^{13}C NMR spectra for compounds **5–13** are those assigned to the iminic carbon of the exocyclic imine groups [C=NXyl or C=N(*p*-MeO-C_6H_4)], which give rise to broad signals in the range 177.6–188.0 ppm, only marginally below those reported by Erker and co-workers for the zwitterionic phosphaboroles CR=C(*p*-tol)PPh_2(C=N^{t}Bu)B(C_6F_5)$_2$ (R = C_6F_5, Me), *ca.* 192 ppm. On the other hand, the carbonyl moiety in **13** gives rise to a resonance at 203.2 ppm, somewhat more deshielded than those reported for similar diazaborolones by Rojas and collaborators (*ca.* 193 ppm).[17] Similarly, signals in the range 158–165 ppm could be easily attributed to the iminic carbon of the endocyclic imine in these compounds.

Dynamic behaviour was observed in the NMR spectra recorded at 298 K for compounds **7a**, **8a**, **9**, **10** and **13**, that is, those derived from the asymmetrical boron and bisboron guanidinates, **2** and **3**. Thus, the compounds with an exocyclic $NH^{i}Pr$ group (*i.e.* **7a**, **8a**, and **13**) displayed rather broad signals assigned to the CH (^{1}H, ^{13}C) and CH_3 (^{1}H) fragments of the other ^{i}Pr group at 298 K. Moreover, the methyne signals are particularly downfield for **7a** and **8a**, at *ca.* 5.25 ppm, and slightly less so for **13** (4.59 ppm), compared to those of other compounds herein reported (usually in the range 3.0–4.2 ppm, see Table 2). This could be explained by weak CH···N hydrogen bond interactions, probably between the methyne group and the exocyclic amine NH(^{i}Pr). In line with this, a short (C5)H···N3 distance of 2.43 Å was measured for **8a** in the solid state, well below the sum of van der Waals radii for these atoms (1.20 Å for H, 1.55 Å for N).[19] Evidence of similar intramolecular CH···N interactions was detected as well for related heterocycles by X-ray diffraction,[20] and/or ^{1}H NMR,[20,21] the latter confirming the deshielding effect of the H atom involved in these interactions. In order to shed some light on the nature of these dynamic processes, variable temperature ^{1}H NMR experiments were carried out for **7a** in toluene-d_8 in the range 253–353 K (see Fig. S5 in the ESI†), as well as for **13** at 333 K in C_6D_6 (Fig. S21(a) in the ESI†) which showed that, upon increasing the temperature, these signals sharpened up progressively to give a somewhat broad septet and a well-defined doublet, for the CH and CH_3 groups of **7a** and **13**, at 353 and 333 K, respectively. Upon cooling down the temperature below 298 K for **7a**, an overall broadening of all signals takes place, especially affecting the aforementioned CH and CH_3 resonances, with the former shifting to higher frequencies, up to 5.66 ppm at 253 K. Unfortunately, below 253 K precipitation of the product precluded further recording at lower temperatures and kinetic parameters concerning these processes could not be calculated. In any event, we believe that, upon cooling down the temperature, the fast rotation of the exocyclic C–N^{i}Pr bond would slow down in the NMR time scale and, at the same time the CH···N interaction would be strengthened,[20] possibly accounting for the latter observations for **7a**.

In the case of bisboron derivatives **9** and **10**, broad signals were also detected for one of the ^{i}Pr groups at 298 K in the ^{1}H NMR. Moreover, compound **9** also showed broad signals for the Cy groups and the inequivalent Me groups of the xylyl fragment, in both the ^{1}H and ^{13}C NMR spectra. Therefore, a variable temperature NMR study was also performed on **9** in toluene-d_8, in the range of temperatures 193–353 K (Fig. S6 in the ESI†). As observed before for **7a**, warming up led to a progressive sharpening of the mentioned broad signals. However, cooling down below 298 K revealed a more complex situation. At 273 K, the methyl resonances of the xylyl group become broader, but below this temperature they sharpen up again, and a new set of signals is clearly evident at 233 K, at similar chemical shifts, most likely attributed to a minor isomer (rotamer) of **9** in a 1 : 3 ratio with respect to the major one. The resonances of one of the ^{i}Pr groups undergo substantial changes as well, not only in line shape, but also in chemical shift. For example, the methyne resonance which gives rise to a septet at 353 K, *ca.* 3.5 ppm, progressively shifts upfield and broadens upon cooling down to 298 K. Below this temperature it sharpens up again down to 233 K, to finally broaden again before splitting into two broad signals at 193 K, at 3.22 and 3.12 ppm, respectively, in a 1 : 4 ratio. At the same time, the Me groups coupled to the latter CH undergo a similar process shifting from 1.25 and 0.96 ppm at 353 K to *ca.* 1.05 and 0.77 ppm, respectively, at 233 K, before broadening up again down to 193 K. All these data clearly indicate the existence of several dynamic processes in solution for compounds **9** and **10**. In this sense, short CH···N contacts were also measured for compound **10** in the solid state, both between the methyne group and the exocyclic N atom, with a (C5)H···N3 distance of 2.48 Å, and also between a Me group and the exocyclic imine, with a (C5)CH_3···N4 distance of 2.44 Å. These interactions alongside inhibited rotation around N–Aryl bonds at low temperatures in the NMR timescale may account for the rotamers detected for compound **9** in solution.

Thermodynamic studies on isonitrile de-insertion in compounds 11 and 12

As mentioned earlier, a fast equilibrium was found in solution between compounds **11** and **12** and the isonitrile de-insertion products, CNAr (Ar = Xyl, *p*-MeO-C_6H_4) and the parent boron guanidinates **3** and **4** (Scheme 5). In both cases, the equilibrium was clearly shifted towards the insertion product at room temperature, which allowed the isolation of these products in high yields. Therefore, we decided to study the effect of temperature on these equilibria by recording ^{1}H NMR spectra in C_6D_6 in the range 298–353 K, which allowed us to calculate the equilibrium constants (K_{eq}) and, by means of Van't Hoff plots ($\ln K_{eq}/T$ *vs.* $1/T$), the thermodynamic parameters, $\Delta H°$ and $\Delta S°$, for the isonitrile de-insertion reaction (Tables S1, S2 and Fig. S1–S4 in the ESI†). Linear regressions nicely fit with our data, giving standard enthalpy and entropy values of 66.6 ± 1.9 kJ mol^{-1} and 175.6 ± 6.0 J mol^{-1} K^{-1} for **11** and 72.2 ± 1.2 kJ mol^{-1} and 170.9 ± 3.7 J mol^{-1} K^{-1} for **12**, respectively. These values are consistent with our experimental observations, as the expected strong entropic contribution implies a shift of the equilibrium towards the de-insertion products upon increasing the temperature.

Some final remarks should be made about these reversible isonitrile and carbonyl insertion/de-insertion equilibria found for the borabicycle derivatives. The optimised structures of **11** and **12**, with a half-chair configuration for the five-membered heterocycle, induced by the steric demands of the BC_8H_{14} moiety, must be less energetically favoured than the pseudo-planar structures found for the BCy_2 derivatives. This will account for the equilibria found for the former BC_8H_{14} derivatives, as opposed to the thermally-stable insertion products obtained for the BCy_2 guanidinates **1–3** (no sign of de-insertion products was detected up to 353 K).

1,2-Insertion reactions of compounds 1–4 with benzaldehydes and CO_2

All the guanidinato compounds, except compound **3**, showed reactivity towards benzaldehyde to give the expected 1,2-insertion products, reminiscent of those reported by Stephan *et al.*[8] and Mikhailov *et al.*[9] with boron amidinates. However, in all cases, the reactions turned out to be in equilibria between the insertion and de-insertion products, most of the times shifted towards the reagents even after employing a great excess of benzaldehyde. For instance, addition of *ca.* 10 equivalents of benzaldehyde to solutions of compound **1** only led to 30% conversion to the insertion product $(Me_2N)C(N^iPr)_2(PhHCO)BCy_2$ (**15**), which could not be isolated and was only identified by ^{1}H NMR (Scheme 6). The reaction of **2** with 2 equivalents of benzaldehyde proceeded slowly at room temperature until an equilibrium was reached after *ca.* 48 h consisting of the two possible N–B insertion products: $\{^iPr(H)N\}C\{N(p\text{-}^tBu\text{-}C_6H_4)\}(N^iPr)(PhHCO)BCy_2$ (**16a**) and $\{^iPr(H)N\}C(N^iPr)\{N(p\text{-}^tBu\text{-}C_6H_4)\}(PhHCO)BCy_2$ (**16b**), in a 7 to 1 ratio with a conversion slightly over 50%. Increasing the temperature up to 60 °C shifted the equilibrium towards the de-insertion products. Luckily, the major insertion product **16a** could be isolated in high yields by carrying out the reaction with 5 equivalents of benzaldehyde in a non-polar solvent such as pentane and crystallisation at −20 °C. Compound **4** reacts with 10 equivalents of benzaldehyde to give the insertion product $\{^iPr(BC_8H_{14})N\}C\{N(p\text{-}Me\text{-}C_6H_4)\}(N^iPr)(PhHCO)BC_8H_{14}$ (**17**), as well as $\{^iPr(H)N\}C\{N(p\text{-}Me\text{-}C_6H_4)\}(N^iPr)(PhHCO)BC_8H_{14}$ (**18**), in a 2 to 1 ratio approx., and *ca.* 60% conversion based on compound **4**. The formation of **18** probably follows from the partial hydrolysis of the exocyclic N–B bond induced by trace amounts of water in the benzaldehyde as increasing the amount of the latter also increased the relative amount of this product (ratio **17** : **18** *ca.* 1 : 2 upon addition of 30 equivalents of benzaldehyde). Unfortunately, none of these products could be isolated. We note as well that the insertion of aldehydes in dialkylboron amidinates reported by Mikhailov and co-workers[9] gave also thermally unstable insertion products, which seems to be related with the relative acidity of the boryl fragment, as

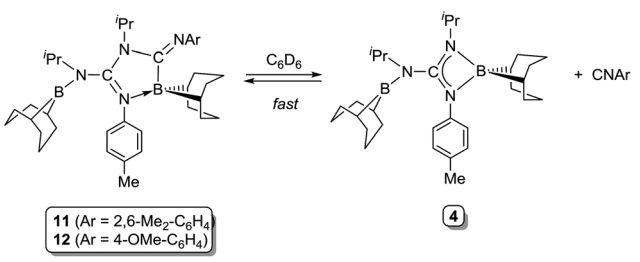

Scheme 5 Isonitrile de-insertion equilibrium for compounds **11** and **12**.

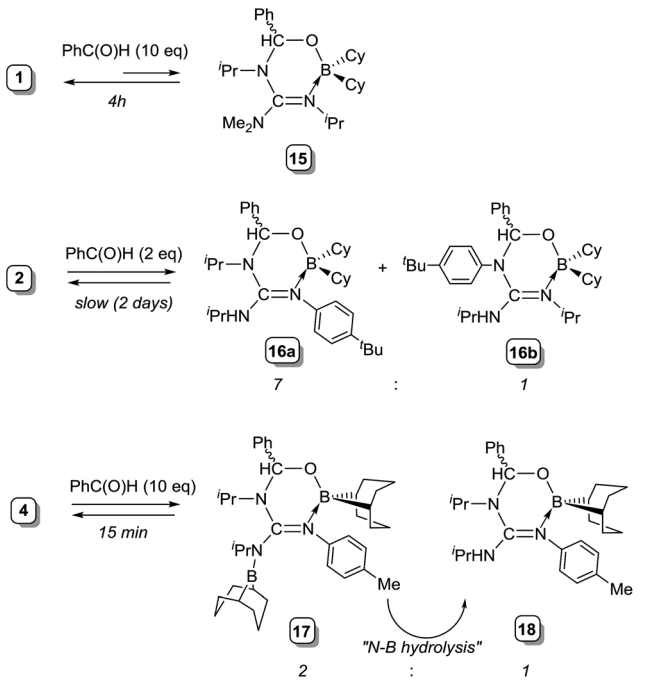

Scheme 6 Reversible 1,2-insertion reactions of **1**, **2** and **4** with benzaldehyde.

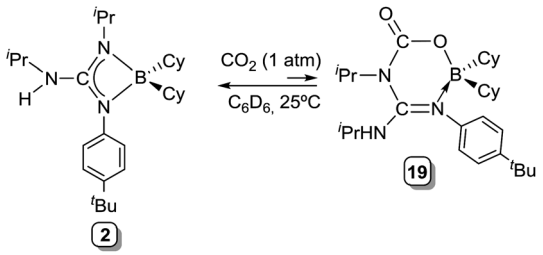

Scheme 7 Reversible 1,2-insertion reaction of **2** and CO_2.

similar insertion products with more acceptor BAr_2 groups (Ar = Ph,[9] C_6F_5[8]), showed higher chemical and thermal stability.

The reactivity of solutions of guanidinato compounds **1–4** was also tested towards CO_2 within sealed NMR tubes. Compounds **1** and **3** did not show evidence of reaction with CO_2 under ambient conditions (1 atm, room temperature). However, the 1,2-insertion product $\{^{i}Pr(H)N\}C\{N(p\text{-}^{t}Bu\text{-}C_6H_4)\}(N^{i}Pr)(CO_2)BCy_2$ (**19**), was detected by ^1H NMR in the reaction of **2** with CO_2 under the same conditions, with a conversion of *ca.* 9% after 15 h at room temperature (Scheme 7). Once more, this reaction turned out to be in equilibrium, and increasing the temperature up to 80 °C resulted in full CO_2 de-insertion to give the parent compound **2**. In this sense, plausible evidence of the formation of small amounts of insertion products (<5%) was also obtained in the reactions of **4** towards CO_2 (1 atm) after *ca.* 15 h at room temperature, which also appear to be in equilibrium with the de-insertion products rather shifted towards the latter. However, these products could be neither isolated nor unambiguously identified. The latter equilibria are not surprising since Stephan and Erker found similar reversible temperature-dependent CO_2 binding in P/B intra- and intermolecular FLP systems.[18]

As already commented for the 1,1-insertion reactions, the 1,2-insertion reactions seem to follow a concerted mechanism from an open-chain form of these boron guanidinates, according to the DFT studies of CO_2 additions to related intramolecular N/B[14] or P/B[18] FLPs. This implies the concomitant formation of N/P–C and B–O bonds. So it can be concluded that increasing the donor capacity of the basic centre and/or the acceptor capacity of the boron centre would lead to more stable insertion products and, in general, more reactive systems. Efforts towards this end are underway in our group, using simple, straightforward synthetic methods for the preparation of new boron amidinates and guanidinates from inexpensive reagents, circumventing the use of C_6F_5 groups on boron. We must note that recent reports prove the validity of this approach, as in the H_2 activation by an "inverse" FLP consisting of a bulky organic superbase and a moderate-to weak boron-based Lewis acid,[22] or the FLP-reactivity of an intramolecular BCy_2-based compound obtained by 1,1-hydroboration of an isonitrile.[23]

Structural characterisation of compounds 15–18

The solid-state structure of compound **16a** was determined by an X-ray diffraction analysis (Fig. 6, Table 4). This compound

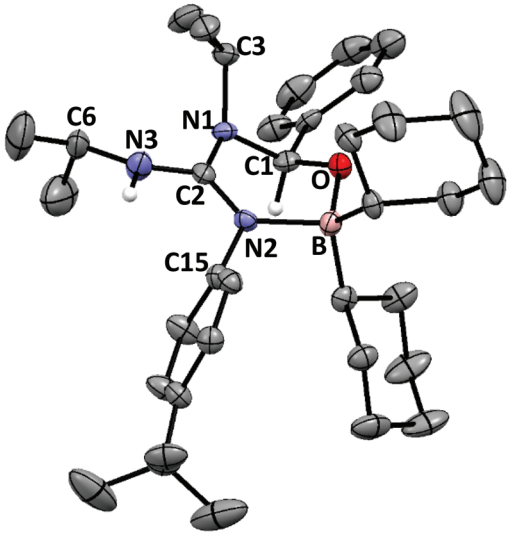

Fig. 6 Molecular structure of compound **16a**: H atoms are omitted for clarity, except for those bound to C1 and N3, and ORTEP ellipsoids are plotted at the 50% probability level.

Table 4 Selected bond lengths (Å) and angles (°) for compound **16a**

B–O	1.474(7)	B–O–C1	112.6(4)
O–C1	1.382(6)	O–C1–N1	109.5(4)
C1–N1	1.495(6)	C1–N1–C2	110.1(4)
N1–C2	1.379(6)	N1–C2–N2	120.0(4)
C2–N2	1.308(6)	N1–C2–N3	119.1(4)
N2–B	1.677(6)	N2–C2–N3	120.9(5)
C2–N3	1.355(7)	C2–N2–B	124.5(4)
N1–C3	1.505(6)	N2–B–O	102.5(4)
N2–C15	1.450(6)	N1–C2–N2/O–C1–N1[a]	56.4

[a] Torsion between the planes.

crystallised in the tetragonal space group $P4_3$. As can be seen, the molecular structure is the expected result of the 1,2-insertion of the double C=O bond in the (^{i}Pr)N–B bond to form a non-planar six-membered heterocycle. Thus, two new single N–C and O–B bonds have been formed, as denoted by the N1–C1 and B–O distances of 1.495(6) and 1.474(7) Å, respectively, whereas the C1–O distance, 1.382(6) Å, is now also consistent with the formulation of a single endocyclic C–O bond. All these bond distances are reminiscent of those found for the related complex $[HC(N^{t}Bu_2)_2(PhCOH)B(C_6F_5)_2]$ reported by Stephan.[8]

The puckered conformation of the six-membered heterocyclic ring is denoted by the sum of the internal angles, *ca.* 680°, far from the theoretical 720° of a planar hexagon. This could be described more accurately as a somewhat distorted half-chair configuration in which the C1 atom is puckered out of the pseudo-planar N1–C2–N2–B–O skeleton (N1–C2–N2–B and C2–N2–B–O torsion angles of only 14.4(7) and 3.9(6)°, respectively). This is corroborated by the wide torsion angle between the N1–C2–N2/O–C1–N1 planes of 56.4°. The C2–N2 distance, of 1.308(6) Å, is consistent with the formulation of a

double C═N bond, although there is still some π delocalisation within the other C–N bonds of the guanidine "CN_3" core, as indicated by C2–N1 and C2–N3 distances, of 1.379(6) and 1.355(7) Å, intermediate between single and double C–N bonds. This observation goes in line with the sum of bond angles about the N atoms: *ca.* 360° for N2, suggesting a sp^2 hybridisation, but *ca.* 346° and 354° for N1 and N3, respectively, indicating some degree of pyramidalisation.

Despite the fact that compound **16a** slowly de-inserts benzaldehyde in solution at room temperature, it could be satisfactorily characterised by multinuclear NMR spectroscopy and the spectra recorded are in quite good agreement with the solid-state structure commented above. Thus, the ^{11}B NMR presented a signature broad signal at 8.0 ppm, suggestive of a tetracoordinate boron. Additionally, the C_1-symmetric structure of the molecule of **16a** gives rise to three distinct signals for each ^{i}Pr group in the ^{1}H NMR spectrum at room temperature (Table 2), a septet (CH) and two doublets (CH_3) for the ^{i}Pr group bound to the endocyclic N atom, and a doublet of septets (CH) and two doublets (CH_3) for the ^{i}Pr group bound to the exocyclic N atom. Likewise, distinct signals were also observed in the carbon-13 NMR spectrum for the ^{i}Pr groups, except for two isochronous Me groups at 23.6 ppm, therefore accounting for a total of five, instead of six signals. Signature singlets at 5.97 ppm (^{1}H) and 82.7 ppm (^{13}C) were attributed to the C*H*(Ph) of the inserted benzaldehyde, in the expected range for similar products of benzaldehyde addition in intramolecular N/B[8] and P/B[24] FLPs. However, the presence of broad signals for the Cy groups in the ^{1}H and ^{13}C NMR spectra, especially in the latter, in which only five signals were detected out of the twelve expected, denoted again the existence of dynamic processes in solution. These observations prompted us to carry out variable-temperature NMR experiments for **16a** in CD_2Cl_2 in the temperature range 290–193 K (Fig. S7 in the ESI†). Thus, upon cooling down from 290 K, an overall broadening of all the signals takes place in the ^{1}H NMR spectra, and at 193 K the splitting of some of the latter gives rise to two sets of signals attributed to two isomers (probably rotamers) of **16a**. Thus, focusing on the singlet at 5.96 ppm, it broadens progressively down to 228 K (coalescence temperature, T_c), before splitting up into two different sharp signals at 193 K, at 5.97 and 5.83 ppm in a 4 to 1 ratio, respectively. Likewise, the signal attributed to the *p*-^{t}Bu group at 1.32 ppm at 290 K splits into two singlets at 1.27 and 1.23 ppm roughly in the same ratio at 193 K. Other signals seem to undergo similar processes, like those from aromatic protons or one of the CH-^{i}Pr moieties. The presence of two isomers at low temperatures probably follows from "freezing" some of the bond rotation processes (exocyclic C–N$H^{i}Pr$, N–aryl, *etc.*) typically fast at room temperature in the NMR time scale.

As already stated before, the other benzaldehyde insertion products were mostly identified by the ^{1}H NMR spectra of the reaction crude and the structural proposal was safely assigned based on the similarity to the fully-characterised compound **16a**. For example, signature singlets *ca.* 6 ppm were assigned in all cases to the *H*C(Ph) of the inserted aldehyde for **15**, **16b**, **17** and **18**. Moreover, the asymmetry of these molecules originated three different signals for each ^{i}Pr group: one for the methyne, CH, in the expected region, *ca.* 3–4 ppm, and two for the methyl groups, *ca.* 1.4–0.4 ppm, detected in all instances, except for the CH_3 groups of the minor isomer **16b**, which were masked by the signals of the major isomer.

In the case of the reaction of **2** with CO_2 to give the insertion product **19**, despite its low conversion, *ca.* 9%, a new set of signals could be easily assigned to the proposed product, with an apparent C_2-symmetry, like the parent guanidinate **2**, most likely due to fast rotation of the exocyclic N$H^{i}Pr$ group as well. As for the regioselectivity of this reaction, we propose that the CO_2 insertion in the ^{i}PrN–B bond based on previous results commented in this paper indicates that this regioisomer is the most stable product in the 1,1- and 1,2-insertion reactions of **2**.

Conclusions

We have studied the N–B insertion reactions of two boron guanidinates, $(Me_2N)C(N^{i}Pr)_2BCy_2$ (**1**) and $\{^{i}Pr(H)N\}C(N^{i}Pr)\{N(p\text{-}^{t}Bu\text{-}C_6H_4)\}BCy_2$ (**2**), and two bisboron guanidinates (2–), $\{^{i}Pr(BCy_2)N\}C(N^{i}Pr)\{N(p\text{-}^{t}Bu\text{-}C_6H_4)\}BCy_2$ (**3**) and $\{^{i}Pr(C_8H_{14}B)N\}C(N^{i}Pr)\{N(p\text{-Me-}C_6H_4)\}BC_8H_{14}$ (**4**), all of them with (cyclo)alkyl groups on boron, towards small unsaturated molecules. Compound **4** was prepared for the first time by deprotonation of a guanidine with a secondary borane, proving the feasibility of this atom-efficient synthetic route instead of the salt metathesis route employed in the other cases. Compounds **1–4** display a chelate coordination mode of the guanidinato ligand to one boron centre, and only compound **1** displayed a fast solvent-dependent equilibrium in solution between a minor monodentate isomer **1-M** and the major chelate **1-C**, relevant from a mechanistic point of view to account for the N–B insertion reactions.

1,1-Insertion of aromatic isonitriles, CNXyl and CN(*p*-MeO-C_6H_4), takes place in all instances to give novel diazaboroles, and in the case of the asymmetrical guanidinates **2–4**, the insertion in the endocyclic (^{i}Pr)N–B bond is always favoured, probably because of the more donor character of this N centre. Four different compounds were structurally characterised in the solid state by X-ray diffraction. Of all the structures, only that derived from **4**, $\{^{i}Pr(BC_8H_{14})N\}C\{N(p\text{-Me-}C_6H_4)\}(N^{i}Pr)(CNXyl)BC_8H_{14}$ (**11**), displayed a puckered five-membered ring as opposed to a pseudo-planar one displayed by BCy_2 derivatives. DFT-optimised structures confirmed that the half-chair arrangement for BC_8H_{14}-derived diazaboroles **11** and **12** has a steric origin induced by the clash of the boron bicyclic group on the neighbouring NAr and C═NAr moieties, a circumstance which seems to be accompanied by a decreased stability of these compounds. This seems to favour the fast temperature-dependent equilibria found in solution between **11** and **12** and the isonitrile de-insertion products, lying far towards the insertion products at room temperature, but being increasingly displaced towards de-insertion upon increasing the temperature

up to 80 °C. Reactions with CO were more sluggish in general, but followed the same tendency found with isonitriles in terms of regioselectivity and equilibria found for the carbonylation product of the BC_8H_{14} derivative **4**.

As for the 1,2-insertion reactions with benzaldehydes and CO_2, when they took place, all turned out to be in equilibria, often shifted towards the de-insertion products. Only one product could be isolated and fully characterised, this being {^{i}Pr(H)N}C{N(*p*-^{t}Bu-C_6H_4)}(N^{i}Pr)(PhHCO)BCy_2 (**16a**).

From these results it can be finally concluded that 1,1- and 1,2-insertion reactions similar to the FLP-type reactivity described by Stephan and co-workers[8] with boron amidinates of the formula $HC(NR)_2B(C_6F_5)_2$ can also be obtained with boron guanidinates straightforwardly prepared from affordable commercial reagents in high yields, with less electron withdrawing groups on boron. The price to pay by reducing the acceptor capacity in the boron centre seems to be a somewhat reduced reactivity of these systems, often detected in the form of insertion/de-insertion equilibria, or precluded insertions under mild conditions. In any event, we believe that increasing the donor ability of the chelate N atoms of the guanidinato ligands, often more basic than their amidinate counterparts due to the presence of an additional exocyclic NR_2 group, and additional fine-tuning of the steric crowding around the B–N bonds could expand the reactivity repertoire of these systems moving away from the C_6F_5 groups on boron, ubiquitous so far in the FLP chemistry. Efforts towards this end are currently underway in our laboratory.

Experimental

General procedures

All manipulations were carried out under dry nitrogen using standard Schlenk and glovebox techniques. Solvents were distilled from appropriate drying agents and stored under N_2 in Schlenk tubes equipped with J. Young-type Teflon stoppers and containing activated molecular sieves (4 Å). Microanalyses were carried out with a LECO CHNS-932 analyser. ATR-FTIR spectra were recorded on a Bruker Tensor 27 spectrophotometer. NMR spectra were recorded on Varian FT-400 and Inova FT-500 spectrometers using standard VARIAN-FT software. Chemical shifts (δ) are given in ppm and coupling constants (J) in Hz. All reagents were purchased from the usual commercial suppliers, except for the guanidine (*p*-Me-C_6H_4N)C(NH^{i}Pr)$_2$[3a] and boron guanidinates (Me$_2$N)C(N^{i}Pr)$_2$BCy_2 (**1**), {^{i}Pr(H)N}C(N^{i}Pr){(*p*-^{t}Bu-C_6H_4)}Cy_2 (**2**) and {^{i}Pr(Cy_2B)N}C(N^{i}Pr){N(*p*-^{t}Bu-C_6H_4)}BCy_2 (**3**),[6] which were prepared according to literature procedures.

Solvent-dependent equilibrium between isomers 1-C and 1-M

Two samples containing compound **1** (0.024 g, 0.07 mmol each) were dissolved in *ca.* 0.8 mL of C_6D_6 and CD_2Cl_2, respectively, charged into NMR tubes equipped with a J. Young valve and their ^{1}H NMR spectra were immediately recorded. The relative isomer ratio was thus measured integrating the methyne signals of each isomer (**1-C** : **1-M** = 89 : 11 in C_6D_6 and 83 : 17 in CD_2Cl_2). Partial spectroscopic data for **1-M**: ^{1}H NMR (400 MHz, C_6D_6): δ 3.82 (sept, 1H, J_{HH} = 6.7 Hz, C*H*-^{i}Pr), 3.49 (sept, 1H, J_{HH} = 6.0 Hz, C*H*-^{i}Pr), 2.67 (s, 6H, N*Me*$_2$). ^{1}H NMR (400 MHz, CD_2Cl_2): δ 3.88 (sept, 1H, J_{HH} = 6.7 Hz, C*H*-^{i}Pr), 3.32 (sept, 1H, J_{HH} = 6.0 Hz, C*H*-^{i}Pr), 2.72 (s, 6H, N*Me*$_2$). The rest of the signals of **1-M** were masked by those of the major isomer **1-C**, although cross-peaks between the CH–CH_3 couples were detected in ^{1}H–^{1}H 2D COSY experiments (see Fig. S8 and S9 in the ESI†).

Preparation of {^{i}Pr(BC_8H_{14})N}C{N(*p*-Me-C_6H_4)}(N^{i}Pr)BC_8H_{14} (4)

A solution of the 9-borabicyclo[3.3.1]nonane dimer, (H-BC_8H_{14})$_2$, (0.625 g, 2.56 mmol) in toluene (10 mL) was added to a solution of (*p*-Me-C_6H_4N)C(NH^{i}Pr)$_2$ (0.586 g, 2.51 mmol) in toluene (10 mL). The resulting solution was stirred for 4 h at room temperature, at which time the solvent was removed under vacuum. The remaining solid was washed with pentane (3 × 10 mL) and dried under vacuum to give compound **4** as a white solid (0.700 g, 59%). Crystals of **4** suitable for an X-ray diffraction study were grown from a concentrated solution of **4** in hexane kept at −20 °C. Anal. calcd for $C_{30}H_{49}B_2N_3$: C, 76.12; H, 10.43; N, 8.88. Found: C, 76.24; H, 10.23; N, 8.71. ^{1}H NMR (500 MHz, C_6D_6): δ 7.09, 6.93 (AA′XX′, 4H, C_6H_4), 3.83 (sept, 1H, J_{HH} = 6.7 Hz, C*H*-^{i}Pr), 3.54 (sept, 1H, J_{HH} = 6.9 Hz, C*H*-^{i}Pr), 2.50–1.20 (m, 28H, 2 × C_8H_{14}), 2.04 (s, 3H, *p*-CH_3-C_6H_4), 1.32 (d, 3H, J_{HH} = 6.7 Hz, C*H*$_3$-^{i}Pr), 1.23 (d, 3H, J_{HH} = 6.7 Hz, C*H*$_3$-^{i}Pr), 0.95 (d, 3H, J_{HH} = 6.9 Hz, C*H*$_3$-^{i}Pr), 0.82 (d, 3H, J_{HH} = 6.9 Hz, C*H*$_3$-^{i}Pr). ^{13}C{^{1}H} NMR (101 MHz, C_6D_6): δ 160.1 (s, *C*N$_3$), 141.0 (s, *ipso-C*-C_6H_4), 135.0 (s, *p-C*-C_6H_4), 129.7, 127.9 (2 × s, *o*,*m-C*-C_6H_4), 53.0, 45.4 (2 × s, 2 × *C*H-^{i}Pr), 34.6, 34.3, 33.5, 33.4, 32.8, 32.6 (6 × s, *C*H_2-BC_8H_{14}), 25.9 (br, *C*H-BC_8H_{14}), 25.1 (s, *C*H_2-BC_8H_{14}), 24.5 (br, *C*H-BC_8H_{14}), 24.4, 24.2 (2 × s, 2 × *C*H$_3$-^{i}Pr), 24.1 (br, *C*H-BC_8H_{14}), 23.8 (s, *C*H$_3$-^{i}Pr), 23.4 (s, *C*H_2-BC_8H_{14}), 22.7 (s, *C*H$_3$-^{i}Pr), 22.2 (s, *C*H_2-BC_8H_{14}), 21.0 (s, *p-C*H_3-C_6H_4). ^{11}B NMR (128 MHz, tol-d_8): δ 53.2 (br, $\Delta\nu_{1/2}$ *ca.* 1100 Hz, tricoordinate B), 12.6 (br, $\Delta\nu_{1/2}$ *ca.* 400 Hz, tetracoordinate B).

Preparation of (Me$_2$N)C(N^{i}Pr)$_2$(CNXyl)BCy_2 (5)

Solid CNXyl (0.066 g, 0.50 mmol) was added to a solution of **1** (0.175 g, 0.50 mmol) in pentane (10 mL). A white suspension containing compound **5** was formed after stirring for 5 min at room temperature. The suspension was further stirred for 3 h to ensure complete reaction. Then, the supernatant was decanted and the solid was washed with cold pentane (2 × 10 mL) and dried under vacuum to give compound **5** as a white solid (0.120 g, 50%). Crystals of **5** suitable for X-ray diffraction were grown from a concentrated solution of **5** in hexane kept at −20 °C. Anal. calcd for $C_{30}H_{51}BN_4$: C, 75.29; H, 10.74; N, 11.71. Found: C, 74.85; H, 10.48; N, 11.64. IR (cm^{-1}): ν 1638 (s, C═N). ^{1}H NMR (500 MHz, C_6D_6): δ 7.12 (d, 2H, J_{HH} = 7.4 Hz, *m*-C_6H_3), 6.94 (t, 1H, J_{HH} = 7.4 Hz, *p*-C_6H_3), 3.57 (sept, 1H, J_{HH} = 6.8 Hz, C*H*-^{i}Pr), 3.32 (sept, 1H, J_{HH} = 6.8 Hz, C*H*-^{i}Pr), 2.46 (s, 6H, *Me*$_2$-Xyl), 2.08 (s, 6H, N*Me*$_2$), 1.95–0.60 (m, 22H, Cy), 1.60 (d, 6H, J_{HH} = 6.8 Hz, C*H*$_3$-^{i}Pr), 1.14 (d, br, 6H, J_{HH} = 6.8 Hz,

CH_3-^{i}Pr). ^{13}C{^{1}H} NMR (101 MHz, C_6D_6): δ 182.6 (s, br, *C* = NXyl), 163.5 (s, *C*N$_3$), 150.3 (s, *ipso-C*-Xyl), 128.1 (s, *m-C*-Xyl), 126.9 (s, br, *o-C*-Xyl), 121.4 (s, *p-C*-Xyl), 47.4, 47.3 (2 × s, 2 × *C*H-^{i}Pr), 41.0 (s, N*Me*$_2$), 30.6, 29.8, 29.4, 28.4 (4 × s, *C*H$_2$-Cy), 22.6 (s, *C*H$_3$-^{i}Pr), 20.6 (s, br, *C*H$_3$-^{i}Pr), 20.0 (s, br, *Me*$_2$-Xyl). ^{11}B NMR (128 MHz, C_6D_6): δ 1.6 (br, $\Delta\nu_{1/2}$ *ca.* 240 Hz, B).

Preparation of (Me$_2$N)C(N^{i}Pr)$_2${CN(*p*-MeO-C$_6$H$_4$)}BCy$_2$ (6)

Compound **6** was prepared in an analogous manner to **5** using compound **1** (0.105 g, 0.30 mmol) and CN(*p*-MeO-C$_6$H$_4$) (0.040 g, 0.30 mmol). It was obtained as a white-orangish solid (0.097 g, 67%). Anal. calcd for $C_{29}H_{49}BN_4O$: C, 72.48; H, 10.28; N, 11.66. Found: C, 72.64; H, 10.06; N, 11.64. IR (cm^{-1}): ν 1638 (s, C═N). ^{1}H NMR (500 MHz, C_6D_6): δ 6.99, 6.95 (AA′BB′, 4H, C_6H_4), 3.59 (sept, 1H, J_{HH} = 6.8 Hz, C*H*-^{i}Pr), 3.38 (s, 3H, OCH_3), 3.30 (sept, 1H, J_{HH} = 6.8 Hz, C*H*-^{i}Pr), 2.08 (s, 6H, N*Me*$_2$), 2.0–0.7 (m, 22H, Cy), 1.60 (d, 6H, J_{HH} = 6.8 Hz, CH_3-^{i}Pr), 1.12 (d, 6H J_{HH} = 6.8 Hz, CH_3-^{i}Pr). ^{13}C{^{1}H} NMR (126 MHz, C_6D_6): δ 182.8 (s, br, *C*═NAr), 163.5 (s, *C*N$_3$), 155.5 (s, *p-C*-Ar), 146.1 (s, *ipso-C*-Ar), 121.9 (s, *m-C*-Ar), 113.7 (s, *o-C*-Ar), 55.1 (s, OCH_3), 47.6, 47.5 (2 × s, 2 × *C*H-^{i}Pr), 40.9 (s, N*Me*$_2$), 31.9 (s, *C*H-Cy), 31.3, 30.0, 30.0, 29.9, 28.6 (5 × s, *C*H$_2$-Cy), 22.4, 20.0 (2 × s, 2 × *C*H$_3$-^{i}Pr). ^{11}B NMR (128 MHz, C_6D_6): δ 1.6 (br, $\Delta\nu_{1/2}$ *ca.* 340 Hz, B).

Reaction of 2 with CNXyl

Method A: Compound **2** (0.045 g, 0.10 mmol) and CNXyl (0.014 g, 0.010 mmol) were dissolved in *ca*. 0.8 mL of C_6D_6 and transferred to an NMR tube equipped with a J. Young valve. The reaction was monitored by ^{1}H NMR, and after 2 h, complete transformation of **2** into a mixture of the insertion compounds {^{i}Pr(H)N}C{N(*p*-^{t}Bu-C$_6$H$_4$)}(N^{i}Pr)(CNXyl)BCy$_2$ (**7a**) and {^{i}Pr(H)N}C(N^{i}Pr){N(*p*-^{t}Bu-C$_6$H$_4$)}(CNXyl)BCy$_2$ (**7b**) in a 6 : 1 ratio was observed. Only compound **7a** could be isolated as a white crystalline solid after removal of the solvent under vacuum and crystallisation in hexane at −20 °C. Method B: Alternatively, compound **7a** could be isolated in higher quantities after stirring a yellow pentane solution (5 mL) containing **2** (0.092 g, 0.20 mmol) and CNXyl (0.027 g, 0.21 mmol) for 4 h. Storage of the latter solution at −20 °C yielded **7a** as a white crystalline solid (0.045 g, 39%). Anal. calcd for $C_{38}H_{59}BN_4$ (**7a**): C, 78.32; H, 10.21; N, 9.61. Found: C, 78.12; H, 10.31; N, 9.69. Spectroscopic data for **7a**: IR (cm^{-1}): ν 3453 (w, N–H), 1649 (s, C═N). ^{1}H NMR (500 MHz, C_6D_6): δ 7.31, 7.23 (AA′XX′, 4H, C_6H_4), 7.14 (d, 2H, J_{HH} = 7.4 Hz, *m*-C$_6H_3$), 6.94 (t, 1H, J_{HH} = 7.4 Hz, *p*-C$_6H_3$), 5.25 (br, 1H, N-C*H*-^{i}Pr), 3.86 (d, 1H, J_{HH} = 9.2 Hz, N*H*), 2.97 (dsept, 1H, J_{HH} = 9.2, 6.3 Hz, NH-C*H*-^{i}Pr), 2.51 (s, 6H, *Me*$_2$-Xyl), 1.95–0.85 (m, 22H, Cy), 1.22 (br, 6H, CH_3-^{i}Pr) 1.17 (s, 9H, CH_3-^{t}Bu), 0.60 (d, 6H, J_{HH} = 6.3 Hz, NH-CH_3-^{i}Pr). ^{1}H NMR (500 MHz, tol-d$_8$, 353 K): δ 7.26, 7.18 (AA′XX′, 4H, C_6H_4), 7.00 (d, 2H, J_{HH} = 7.5 Hz, *m*-C$_6H_3$), 6.79 (t, 1H, J_{HH} = 7.5 Hz, *p*-C$_6H_3$), 5.23 (sept, br, J_{HH} *ca*. 7.0 Hz, 1H, N-C*H*-^{i}Pr), 3.88 (d, 1H, J_{HH} = 9.2 Hz, N*H*), 2.99 (dsept, 1H, J_{HH} = 9.2, 6.4 Hz, NH-C*H*-^{i}Pr), 2.38 (s, 6H, 2,6-*Me*$_2$-X), 1.80–0.75 (m, 22H, Cy), 1.25 (d, 6H, J_{HH} = 7.2 Hz, CH_3-^{i}Pr), 1.16 (s, 9H, CH_3-^{t}Bu), 0.68 (d, 6H, J_{HH} = 6.4 Hz, NH-CH_3-^{i}Pr). ^{1}H NMR (500 MHz, tol-d$_8$, 298 K): δ 7.26, 7.18 (AA′XX′, 4H, C_6H_4), 7.06 (d, 2H, J_{HH} = 7.3 Hz, *m*-C$_6H_3$), 6.85 (t, 1H, J_{HH} = 7.3 Hz, *p*-C$_6H_3$), 5.28 (br, 1H, N-C*H*-^{i}Pr, $\Delta\nu_{1/2}$ *ca.* 75 Hz), 3.86 (d, 1H, J_{HH} = 9.2 Hz, N*H*), 2.95 (dsept, 1H, J_{HH} = 9.2, 6.4 Hz, NH-C*H*-^{i}Pr), 2.44 (s, 6H, *Me*$_2$-Xyl), 1.85–0.80 (m, 22H, Cy), 1.22 (br, 6H, CH_3-^{i}Pr) 1.17 (s, 9H, CH_3-^{t}Bu), 0.63 (d, 6H, J_{HH} = 6.4 Hz, NH-CH_3-^{i}Pr). ^{1}H NMR (500 MHz, tol-d$_8$, 253 K): δ 7.25, 7.16 (AA′XX′, 4H, C_6H_4), 7.11 (d, 2H, J_{HH} = 7.3 Hz, *m*-C$_6H_3$), 6.91 (t, 1H, J_{HH} = 7.3 Hz, *p*-C$_6H_3$), 5.66 (br, 1H, N-C*H*-^{i}Pr, $\Delta\nu_{1/2}$ *ca*. 160 Hz), 3.86 (br, 1H N*H*), 2.92 (br, 1H, NH-C*H*-^{i}Pr), 2.49 (s, 6H, *Me*$_2$-Xyl), 2.00–0.85 (m, 22H, Cy), 1.22 (br, 6H, CH_3-^{i}Pr) 1.14 (s, 9H, CH_3-^{t}Bu), 0.59 (d, br, 6H, J_{HH} *ca.* 6.4 Hz, NH-CH_3-^{i}Pr). The signal for the Me groups of one of the ^{i}Pr groups was not detected, obscured by the signals owing to Cy groups. ^{13}C{^{1}H} NMR (101 MHz, C_6D_6): δ 177.6 (s, br, *C*═NXyl), 158.0 (s, *C*N$_3$), 149.6, 149.5 (2 × s, *p-C*-C$_6$H$_4$ + *ipso-C*-Xyl), 140.0 (s, *ipso-C*-C$_6$H$_4$), 128.1 (s, *m-C*-Xyl), 127.1 (s, *o*/*m-C*-C$_6$H$_4$), 126.6 (s, *o-C*-Xyl), 125.9 (s, *m*/*o-C*-C$_6$H$_4$), 121.2 (s, *p-C*-Xyl), 46.1 (s, NH-*C*H-^{i}Pr), 41.8 (br, N-*C*H-^{i}Pr), 34.5 (s, *C*-^{t}Bu), 31.4 (s, *C*H$_3$-^{t}Bu), 30.8 (s, br, *C*H-Cy), 29.8, 29.5, 29.4, 28.5 (4 × s, 4 × br, *C*H$_2$-Cy), 23.1 (s, NH-*C*H$_3$-^{i}Pr), 21.3 (s, N-*C*H$_3$-^{i}Pr), 20.1 (s, *Me*$_2$-Xyl). ^{11}B NMR (128 MHz, tol-d$_8$): δ 0.6 (br, $\Delta\nu_{1/2}$ *ca.* 600 Hz, B). Partial spectroscopic data for **7b**: ^{1}H NMR (500 MHz, C_6D_6): δ 3.82 (sept, 1H, J_{HH} = 7.2 Hz, N-C*H*-^{i}Pr), 3.55 (d, 1H, J_{HH} = 8.9 Hz, N*H*), 2.74 (dsept, 1H, J_{HH} = 8.9, 6.4 Hz, NH-C*H*-^{i}Pr), 2.07 (s, 6H, *Me*$_2$-Xyl), 1.14 (d, 6H, J_{HH} = 7.2 Hz, N-CH_3-^{i}Pr), 1.12 (s, 9H, CH_3-^{t}Bu), 0.52 (d, 6H, J_{HH} = 6.4 Hz, NH-CH_3-^{i}Pr).

Reaction of 2 with CN(*p*-MeO-C$_6$H$_4$)

Method A: Compound **2** (0.045 g, 0.10 mmol) and CN(*p*-MeO-C$_6$H$_4$) (0.014 g, 0.10 mmol) were dissolved in *ca*. 0.8 mL of C_6D_6 and transferred to an NMR tube equipped with a J. Young valve. The reaction was monitored by ^{1}H NMR, and after 2 h at room temperature, complete transformation of **2** into a mixture of the insertion compounds {^{i}Pr(H)N}C{N(*p*-^{t}Bu-C$_6$H$_4$)}(N^{i}Pr){CN(*p*-MeO-C$_6$H$_4$)}BCy$_2$ (**8a**) and {^{i}Pr(H)N}C(N^{i}Pr){N(*p*-^{t}Bu-C$_6$H$_4$)}{CN(*p*-MeO-C$_6$H$_4$)}BCy$_2$ (**8b**) in a 3 : 1 ratio was observed. Only **8a** could be isolated as a white-yellowish crystalline solid after crystallisation in a concentrated solution in pentane of the reaction mixture kept at −20 °C (0.020 g, 34%). These crystals were also suitable for an X-ray diffraction analysis. Method B: Alternatively, **8a** can be prepared in a 0.20 mmol scale with similar yields by the reaction of **2** and CN(*p*-MeO-C$_6$H$_4$) in pentane, isolated as well by crystallisation at −20 °C. Anal. calcd for $C_{37}H_{57}BN_4O$ (**8a**): C, 76.01; H, 9.83; N, 9.58. Found: C, 75.72; H, 9.70; N, 9.39. Spectroscopic data for **8a**: IR (cm^{-1}): ν 3346 (w, N–H), 1638 (s, C═N). ^{1}H NMR (400 MHz, C_6D_6): δ 7.28, 7.23 {AA′XX′, 4H, C_6H_4(^{t}Bu)}, 7.15, 6.98 {AA′XX′, 4H, C_6H_4(OMe)}, 5.20 (br, 1H, N-C*H*-^{i}Pr), 3.79 (d, 1H, J_{HH} = 9.4 Hz, N*H*), 3.38 (s, 3H, OCH_3), 2.96 (dsept, 1H, J_{HH} = 9.4, 6.4 Hz, NH-C*H*-^{i}Pr), 2.0–0.9 (m, 22H, Cy), 1.33 (d, br, 6H, J_{HH} = 6.8 Hz, CH_3-^{i}Pr), 1.16 (s, 9H, CH_3-^{t}Bu), 0.61 (d, J_{HH} = 6.4 Hz, CH_3-^{i}Pr). ^{13}C{^{1}H} NMR (101 MHz, C_6D_6): δ 180.0 {s, br, *C*═N-(*p*-MeO-C$_6$H$_4$)}, 158.2 (s, *C*N$_3$), 155.7 {s, *p-C*-C$_6$H$_4$(OMe)}, 149.9 {s, *p-C*-C$_6$H$_4$(^{t}Bu)}, 145.8 {s, *ipso-C*-C$_6$H$_4$(OMe)}, 140.1 {s, *ipso-C*-C$_6$H$_4$(^{t}Bu)}, 127.8, 126.0

{2 × s, *o*,*m*-*C*-$C_6H_4(^tBu)$}, 122.2 {s, *m*-*C*-$C_6H_4(OMe)$}, 113.8 {s, *o*-*C*-$C_6H_4(OMe)$}, 55.1 (s, O*C*H_3), 46.3 (s, NH-*C*H-^{i}Pr), 42.9 (br, N-*C*H-^{i}Pr), 34.5(s, *C*-^{t}Bu), 32.1 (br, *C*H-Cy), 31.4 (s, *C*H_3-^{t}Bu), 30.3, 30.1, 30.0, 29.9, 28.7 (5 × s, *C*H_2-Cy), 23.2 (s, NH-*C*H_3-^{i}Pr), 21.1 (s, N-*C*H_3-^{ti}Pr). ^{11}B NMR (128 MHz, C_6D_6): δ 0.7 (br, $\Delta\nu_{1/2}$ *ca.* 580 Hz, B). Partial spectroscopic data for **8b**: ^{1}H NMR (500 MHz, C_6D_6): δ 7.35–7.25 {AA′XX′, 4H, $C_6H_4(^tBu)$}, 6.92, 6.83 {AA′XX′, 4H, $C_6H_4(OMe)$}, 3.78 (sept, 1H, J_{HH} = 7.2 Hz, N-C*H*-^{i}Pr), 3.69 (d, 1H, J_{HH} = 9.2 Hz, N*H*), 3.30 (s, 3H, OCH_3), 2.82 (dsept, 1H, J_{HH} = 9.2, 6.4 Hz, NH-C*H*-^{i}Pr), 1.13 (s, 9H, CH_3-^{t}Bu), 1.12 (d, 6H, J_{HH} = 7.2 Hz, CH_3-^{i}Pr), 0.61 (d, J_{HH} = 6.4 Hz, CH_3-^{i}Pr).

Preparation of {^{i}Pr(BCy$_2$)N}C{N(*p*-^{t}Bu-C$_6$H$_4$)}(N^{i}Pr)(CNXyl)BCy$_2$ (9)

Neat CNXyl (0.014 g, 0.10 mmol) was added to a suspension of compound **3** (0.063 g, 0.10 mmol) in hexane (5 mL). The mixture was stirred for 2 days at room temperature and a white suspension containing **9** was finally obtained. After decanting the mother liquor, washing with more cold hexane (2 × 5 mL), and drying under vacuum, compound **9** was obtained as a white solid (0.050 g, 66%). Anal. calcd for $C_{50}H_{80}B_2N_4$: C, 79.14; H, 10.63; N, 7.38. Found: C, 79.13; H, 10.39; N, 7.07. IR (cm^{-1}): ν 1634 (m, C═N). ^{1}H NMR (400 MHz, C_6D_6): δ 7.33, 7.26 (AA′XX′, 4H, C_6H_4), 7.16–7.10 (m, 2H, *m*-C_6H_3), 6.95 (t, J_{HH} = 7.4 Hz, 1H, *p*-C_6H_3), 4.10 (sept, 1H, J_{HH} = 6.7 Hz, C*H*-^{i}Pr), 3.40 (br, 1H, C*H*-^{i}Pr), 2.59, 2.52 (2 × s, 2 × 3H, *Me*$_2$-Xyl), 2.20–0.50 (m, 44H, Cy), 1.79, 1.75 (2 × d, 2 × 3H, J_{HH} = 6.7 Hz, 2 × CH_3-^{i}Pr), *ca.* 1.2 (vbr, 3H, CH_3-^{i}Pr), 1.11 (s, 9H, CH_3-^{t}Bu), *ca.* 0.9 (vbr, 3H, CH_3-^{i}Pr). ^{1}H NMR (500 MHz, tol-d$_8$, 353 K): δ 7.28, 7.25 (AA′XX′, 4H, C_6H_4), 7.03–6.99 (m, 2H, *m*-C_6H_3), 6.81 (t, 1H, J_{HH} = 7.5 Hz, *p*-C_6H_3), 4.12 (sept, 1H, J_{HH} = 6.7 Hz, C*H*-^{i}Pr), 3.49 (≈sept, 1H, J_{HH} ≈ 6.8 Hz, C*H*-^{i}Pr), 2.49, 2.44 (2 × s, 2 × 3H, *Me*$_2$-Xyl), 2.10–0.65 (m, 44H, Cy), 1.79, 1.74 (2 × d, 2 × 3H, J_{HH} = 6.7 Hz, CH_3-^{i}Pr), 1.25 (d, 3H, J_{HH} = 6.7 Hz, CH_3-^{i}Pr), 1.12 (s, 9H, CH_3-^{t}Bu), 0.96 (d, J_{HH} = 6.4 Hz, 3H, CH_3-^{i}Pr). ^{1}H NMR (500 MHz, tol-d$_8$, 298 K): δ 7.29, 7.24 (AA′XX′, 4H, C_6H_4), 7.09–7.03 (m, 2H, *m*-C_6H_3), 6.87 (t, J_{HH} = 7.5 Hz, 1H, *p*-C_6H_3), 4.10 (sept, 1H, J_{HH} = 6.7 Hz, C*H*-^{i}Pr), 3.40 (br, $\Delta\nu_{1/2}$ *ca.* 50 Hz, 1H, C*H*-^{i}Pr), 2.55, 2.49 (2 × s, 2 × br, 2 × 3H, *Me*$_2$-Xyl), 2.30–0.40 (m, 44H, Cy), 1.79, 1.74 (2 × d, 2 × 3H, J_{HH} = 6.7 Hz, CH_3-^{i}Pr), 1.10 (s, 9H, CH_3-^{t}Bu). Broad signals attributed to CH_3-^{i}Pr could not be detected due to overlapping with Cy signals. ^{1}H NMR (500 MHz, tol-d$_8$, 233 K): δ 7.40–7.20 (m, br, 4H, C_6H_4), 7.17–7.09 (m, 2H, *m*-C_6H_3), 6.97 (t, J_{HH} = 7.5 Hz, 1H, *p*-C_6H_3), 4.05 (sept, br, 1H, J_{HH} *ca.* 6.5 Hz, C*H*-^{i}Pr), 3.22 (br, $\Delta\nu_{1/2}$ *ca.* 30 Hz, 1H, C*H*-^{i}Pr), 2.67, 2.51 (2 × s, 2 × br, 2 × 3H, *Me*$_2$-Xyl), 2.40–0.40 (m, 44H, Cy), 1.77, 1.73 (2 × d, J_{HH} *ca.* 6.5 Hz, 2 × CH_3-^{i}Pr), 1.06 (s, 9H, CH_3-^{t}Bu), 1.05 (d, br, 3H, CH_3-^{i}Pr), 0.77 (d, br, 3H, J_{HH} *ca.* 6 Hz, CH_3-^{i}Pr). Signals at 2.68 and 2.49 (*Me*$_2$-Xyl) and 1.09 (CH_3-^{t}Bu) are attributed to a minor rotamer of this compound (ratio minor/major rotamer *ca.* 1 : 3 at 233 K). ^{1}H NMR (500 MHz, tol-d$_8$, 193 K): δ 7.45–6.90 (m, br, 7H, Ar), 4.02, 3.12 (2 × br, 2 × 1H, 2 × C*H*-^{i}Pr), 2.73, 2.55 (2 × br, 2 × 3H, *Me*$_2$-Xyl), 2.50–0.50 (m, 44H, Cy), 1.76, 1.74 (2 × br, 2 × 3H, 2 × CH_3-^{i}Pr), 1.05 (s, 9H, CH_3-^{t}Bu), 1.00, 0.74 (2 × br, 2 × 3H, 2 × CH_3-^{i}Pr). Broad signals at 3.22 (C*H*-^{i}Pr), 2.70 and 2.62 ppm are attributed to a minor rotamer (ratio minor/major rotamer *ca.* 1 : 4 at 193 K). ^{13}C{^{1}H} NMR (101 MHz, C_6D_6): δ 181.7 (s, br, *C*═NXyl), 164.9 (s, *C*N$_3$), 150.4, 149.7 (2 × s, *p*-*C*-C_6H_4 + *ipso*-*C*-Xyl), 138.9 (s, *ipso*-*C*-C_6H_4), 128.3 (s, *o*,*m*-*C*-C_6H_4), 127.9 (s, *m*-*C*-Xyl), 125.5 (s, *m*,*o*-*C*-C_6H_4), 121.7 (s, *p*-*C*-Xyl), 55.3 (br, *C*H-^{i}Pr), 48.9 (s, *C*H-^{i}Pr), 34.9–27.2 (Cy), 34.5 (s, *C*-^{t}Bu), 31.3 (s, *C*H_3-^{t}Bu), 24.5, 24.0, 22.0 (3 × br, CH_3-^{i}Pr), 20.8, 19.7 (2 × br). ^{11}B NMR (128 MHz, tol-d$_8$): δ 49.5 (br, $\Delta\nu_{1/2}$ *ca.* 500 Hz, tricoordinate B), 1.5 (br, $\Delta\nu_{1/2}$ *ca.* 600 Hz, tetracoordinate B).

Preparation of {^{i}Pr(BCy$_2$)N}C{N(*p*-^{t}Bu-C$_6$H$_4$)}(N^{i}Pr){CN(*p*-MeO-C$_6$H$_4$)}BCy$_2$ (10)

Compound **10** was prepared in a similar manner to **9**, employing compound **3** (0.090 g, 0.14 mmol), CN(*p*-MeO-C_6H_4) (0.022 g, 0.16 mmol) and hexane (4 mL). Compound **10** was thus obtained as a white solid (0.065 g, 60%) after stirring for 4 days at room temperature and a similar workup to that used for compound **9**. Crystals of **10** suitable for an X-ray diffraction analysis were grown from a concentrated solution of **10** in hexane at −20 °C. Anal. calcd for $C_{49}H_{78}B_2N_4O$: C, 77.36; H, 10.33; N, 7.36. Found: C, 77.47; H, 10.15; N, 7.17. IR (cm^{-1}): ν 1652 (m, C═N). ^{1}H NMR (400 MHz, C_6D_6): δ 7.23 {s, 4H, $C_6H_4(^tBu)$}, 7.08, 6.99 {AA′XX′, 4H, $C_6H_4(OMe)$}, 4.07 (sept, 1H, J_{HH} = 6.7 Hz, C*H*-^{i}Pr), 3.46 (m, 1H, J_{HH} = 6.9, 6.6 Hz, C*H*-^{i}Pr), 3.39, (s, 3H, OCH_3), 2.10–0.35 (m, 44H, Cy), 1.78, 1.77 (2 × d, 2 × 3H, J_{HH} = 6.7 Hz, 2 × CH_3-^{i}Pr), *ca.* 1.25 (d, br, 3H, J_{HH} = 6.9 Hz, CH_3-^{i}Pr), 1.12 (s, 9H, CH_3-^{t}Bu), 0.92 (d, br, 3H, J_{HH} = 6.6 Hz, CH_3-^{i}Pr). ^{13}C{^{1}H} NMR (101 MHz, C_6D_6): δ 181.9 {s, br, *C*═N-(*p*-MeO-C_6H_4)}, 164.5 (s, *C*N$_3$), 155.9 {s, *p*-*C*-C_6H_4(OMe)}, 150.5 {s, *p*-*C*-$C_6H_4(^tBu)$}, 145.5 {s, *ipso*-*C*-C_6H_4(OMe)}, 139.0 {s, *ipso*-*C*-$C_6H_4(^tBu)$}, 128.5, 125.4 {2 × s, *o*,*m*-*C*-$C_6H_4(^tBu)$}, 121.8 {s, *m*-*C*-C_6H_4(OMe)}, 113.8 {s, *o*-*C*-C_6H_4(OMe)}, 55.2 (s, OCH_3), 54.3 (br, *C*H-^{i}Pr), 49.3 (s, *C*H-^{i}Pr), 34.8 (s, *C*H-Cy), 34.5 (s, *C*-^{t}Bu), 33.6, 32.9, 32.1 (3 × s, 3 × *C*H-Cy), 31.4 (s, *C*H_3-^{t}Bu), 30.6–27.3 (*C*H_2-Cy), 25.2, 23.5 (2 × s, 2 × br, 2 × *C*H_3-^{i}Pr), 21.7, 21.2 (2 × s, 2 × *C*H_3-^{i}Pr). ^{11}B NMR (128 MHz, C_6D_6): δ *ca.* 51 (vbr, tricoordinate B), *ca.* −2 (vbr, tetracoordinate B).

Preparation of {^{i}Pr(BC$_8$H$_{14}$)N}C{N(*p*-Me-C$_6$H$_4$)}(N^{i}Pr)(CNXyl)BC$_8$H$_{14}$ (11)

A yellow hexane suspension (4 mL) containing compound **4** (0.095 g, 0.20 mmol) and CNXyl (0.030 g, 0.22 mmol) was stirred for 2 h at room temperature to yield a suspension containing compound **11**. After a similar workup to that of compound **9**, compound **11** was obtained as a light yellow solid (0.106 g, 88%). Crystals of **11** suitable for an X-ray diffraction analysis were grown from a concentrated solution of **11** in hexane at −20 °C. Anal. calcd for $C_{39}H_{58}B_2N_4$: C, 77.49; H, 9.67; N, 9.27. Found: C, 77.11; H, 9.59; N, 9.08. IR (cm^{-1}): ν 1648 (m, C═N). ^{1}H NMR (500 MHz, C_6D_6, 298 K): δ 7.27–6.85 (m, 7H, Ar), 4.15 (sept, 1H, J_{HH} = 6.7 Hz, C*H*-^{i}Pr), 2.97 (sept, 1H, J_{HH} = 6.7 Hz, C*H*-^{i}Pr), 2.54, 2.52 (2 × s, 2 × 3H, *Me*$_2$-Xyl), 2.00 (s, 3H, *p*-*Me*-C_6H_4), 2.25–1.10 (m, 28H, 2 × C_8H_{14}), 1.79, 1.72, 0.95, 0.41 (4 × d, 4 × 3H, J_{HH} = 6.7 Hz, 4 × CH_3-^{i}Pr).

^{1}H NMR (500 MHz, CD_2Cl_2, 253 K): δ 7.20–7.08 (m, 3H, C_6H_4), 6.99–6.93 (m, 2H, *m*-C_6H_3), 6.92 (m, 1H, C_6H_4), 6.75 (t, 1H, J_{HH} = 7.4 Hz, *p*-C_6H_3), 4.22 (sept, 1H, J_{HH} = 6.7 Hz, C*H*-^{i}Pr), 3.21 (sept, 1H, J_{HH} = 6.7 Hz, C*H*-^{i}Pr), 2.34 (s, 3H, *p*-*Me*-C_6H_4), 2.26 (s, 6H, *Me*$_2$-Xyl), 2.20–0.60 (m, 28H, 2 × C_8H_{14}), 1.74 (d, 3H, J_{HH} = 6.7 Hz, CH_3-^{i}Pr), 1.69 (d, 3H, J_{HH} = 6.7 Hz, CH_3-^{i}Pr), 1.24 (d, 3H, J_{HH} = 6.9 Hz, CH_3-^{i}Pr), 0.50 (d, 3H, J_{HH} = 6.7 Hz, CH_3-^{i}Pr). ^{13}C{^{1}H} NMR (126 MHz, CD_2Cl_2, 253 K): δ 188.0 (s, br, *C*═NXyl), 162.7 (s, *C*N$_3$), 149.2 (s, *ipso-C*-Xyl), 139.8 (s, *ipso-C*-C_6H_4), 137.0 (s, *p-C*-C_6H_4), 129.6, 129.5 (2 × s, *o*,*m-C*-C_6H_4), 128.1 (s, *m-C*-Xyl), 127.9 (s, *o*,*m-C*-C_6H_4), 127.7 (s, *m-C*-Xyl), 127.3 (s, *o*,*m-C*-C_6H_4), 127.2 (s, *o-C*-Xyl), 126.1 (s, *o-C*-Xyl), 121.1 (s, *p-C*-Xyl), 54.4, 48.2 (2 × s, 2 × *C*H-^{i}Pr), 34.4, 33.5, 33.1, 32.1, 32.0, 32.0, 31.4, 30.6 (8 × s, *C*H$_2$-BC_8H_{14}), 29.3, 24.8 (2 × br, *C*H-BC_8H_{14}), 24.4 (s, *C*H$_2$-BC_8H_{14}), 24.3 (br, *C*H-BC_8H_{14}), 24.3 (s, *C*H$_3$-^{i}Pr), 24.0 (s, *C*H$_2$-BC_8H_{14}), 24.0 (s, *C*H$_3$-^{i}Pr), 23.2 (s, *C*H$_2$-BC_8H_{14}), 22.5 (s, *C*H$_3$-^{i}Pr), 22.3 (s, *C*H$_2$-BC_8H_{14}), 21.0 (s, *p-C*H$_3$-C_6H_4), 20.7 (br, *C*H-BC_8H_{14}), 20.2 (s, *C*H$_3$-^{i}Pr), 19.5, 19.4 (2 × s, *Me*$_2$-Xyl). ^{11}B NMR (128 MHz, CD_2Cl_2, 298 K): δ 56.3 (br, $\Delta\nu_{1/2}$ *ca.* 1200 Hz, tricoordinate B), *ca.* 2.5 (br, $\Delta\nu_{1/2}$ *ca.* 400 Hz, tetracoordinate B).

Preparation of {^{i}Pr(BC_8H_{14})N}C{N(*p*-Me-C_6H_4)}(N^{i}Pr){CN(*p*-MeO-C_6H_4)}BC_8H_{14} (12)

Compound **12** was prepared in a similar manner to that of **11**, from compound **4** (0.095 g, 0.20 mmol) and CN(*p*-MeO-C_6H_4) (0.030 g, 0.22 mmol), and isolated as a pale yellow solid (0.100 g, 83%). Anal. calcd for $C_{38}H_{56}B_2N_4O$: C, 75.25; H, 9.31; N, 9.24. Found: C, 74.94; H, 9.25; N, 9.10. IR (cm^{-1}): ν 1633 (m, C═N). ^{1}H NMR (400 MHz, C_6D_6): δ 7.26 {m, 1H, *o*,*m*-C_6H_4(Me)}, 7.10–6.90 (m, 7H, Ar), 4.10 (sept, *J* = 6.7 Hz, 1H), 3.39 (s, 3H, OCH_3), 2.87 (sept, 1H, J_{HH} = 6.7 Hz, C*H*-^{i}Pr), 2.40–1.10 (m, 28H, 2 × C_8H_{14}), 2.01 (s, 3H, *p*-*Me*-C_6H_4), 1.78, 1.71, 0.98, 0.35 (4 × d, 4 × 3H, J_{HH} = 6.7 Hz, 4 × CH_3-^{i}Pr). ^{13}C{^{1}H} NMR (101 MHz, C_6D_6): δ 185.4 (s, br, *C*═NAr′), 162.7 (s, *C*N$_3$), 156.0 {s, *p-C*-C_6H_4(OMe)}, 145.9 {s, *ipso-C*-C_6H_4(OMe)}, 140.7 {s, *ipso-C*-C_6H_4(Me)}, 136.9 {s, *p-C*-C_6H_4(Me)}, 129.6, 129.6, 128.7, 128.5 {4 × s, *o*,*m-C*-C_6H_4(Me)}, 121.2 {s, br, *m-C*-C_6H_4(OMe)}, 114.5 {s, *o-C*-C_6H_4(OMe)}, 55.2 (s, O*C*H$_3$), 54.3, 48.6 2 (2 × s, 2 × *C*H-^{i}Pr), 34.5, 33.6, 33.5, 32.6, 32.4, 32.1, 31.9, 31.5 (8 × s, *C*H$_2$-BC_8H_{14}), 30.9, 25.1 (2 × br, *C*H-BC_8H_{14}), 25.0, 24.6 (2 × s, *C*H$_2$-BC_8H_{14}), 24.5 (br, *C*H-BC_8H_{14}), 24.3, 23.7 (2 × s, 2 × *C*H$_3$-^{i}Pr) 23.2 (s, *C*H$_2$-BC_8H_{14}), 22.8 (s, *C*H$_3$-^{i}Pr), 22.6 (s, *C*H$_2$-BC_8H_{14}), 21.1 (br, *C*H-BC_8H_{14}), 20.9 (s, *p-C*H$_3$-C_6H_4), 19.9 (s, *C*H$_3$-^{i}Pr). ^{11}B NMR (128 MHz, C_6D_6): δ 52.5 (br, $\Delta\nu_{1/2}$ *ca.* 1200 Hz, tricoordinate B), *ca.* 2.7 (br, $\Delta\nu_{1/2}$ *ca.* 600 Hz, tetracoordinate B).

Preparation of {^{i}Pr(H)N}C{N(*p*-^{t}Bu-C_6H_4)}(N^{i}Pr)(CO)BCy_2 (13)

A toluene solution (10 mL) containing compound **2** (0.120 g, 0.27 mmol) was charged into a glass vessel equipped with a J. Young stopper, placed under a CO atmosphere (*ca.* 4 atm) by the freeze–pump–thaw procedure, and stirred at 40 °C for 3 days. Then, the solvent was removed under vacuum, and the remaining viscous solid was dissolved in hexane and kept at −20 °C. A white precipitate was thus obtained; the mother liquor was decanted and the solid was washed with cold hexane (2 × 5 mL). After drying under vacuum, compound **13** was obtained as a white solid (0.030 g, 23%). Anal. calcd for $C_{30}H_{50}BN_3O$: C, 75.14; H, 10.51; N, 8.76. Found: C, 75.21; H, 10.20; N, 8.59. IR (cm^{-1}): ν 3294 (m, br, N–H), 1674 (s, C═O). ^{1}H NMR (400 MHz, C_6D_6): δ 7.26, 7.23 (AA′BB′, 4H, *p*-^{t}Bu-C_6H_4), 4.59 (br, 1H, N-C*H*-^{i}Pr), 4.05 (d, 1H, J_{HH} = 9.3 Hz, N*H*), 3.06 (dsept, 1H, J_{HH} = 9.3, 6.4 Hz, NH-C*H*-^{i}Pr), 2–0–0.9 (m, 22H, Cy), 1.19 (d, br, 6H, J_{HH} *ca.* 7 Hz, CH_3-^{i}Pr), 1.18 (s, 9H, CH_3-^{t}Bu), 0.61 (d, J_{HH} = 6.4 Hz, CH_3-^{i}Pr). ^{1}H NMR (400 MHz, C_6D_6, 333 K): δ 7.25, 7.25 (AA′BB′, 4H, *p*-^{t}Bu-C_6H_4), 4.56 (sept, J_{HH} *ca.* 7.0 Hz, 1H, N-C*H*-^{i}Pr), 3.94 (d, 1H, J_{HH} = 9.3 Hz, N*H*), 3.08 (dsept, 1H, J_{HH} = 9.3, 6.4 Hz, NH-C*H*-^{i}Pr), 2–0–0.9 (m, 22H, Cy), 1.20 (d, 6H, J_{HH} *ca.* 7 Hz, CH_3-^{i}Pr), 1.19 (s, 9H, CH_3-^{t}Bu), 0.63 (d, J_{HH} = 6.4 Hz, CH_3-^{i}Pr). ^{13}C{^{1}H} NMR (126 MHz, C_6D_6): δ 203.2 (s, br, *C*═O), 158.2 (s, *C*N$_3$), 149.7 (s, *p-C*-C_6H_4), 139.8 (s, *ipso-C*-C_6H_4), 126.4, 126.1 (2 × s, *o*,*m-C*-C_6H_4), 46.5 (s, N-*C*H-^{i}Pr), 41.0 (br, NH-*C*H-^{i}Pr), 34.6 (s, *C*-^{t}Bu), 31.4 (s, *C*H$_3$-^{t}Bu), 30.8 (br, *C*H-Cy), 30.1, 29.8, 29.8, 29.6, 28.5 (5 × s, *C*H$_2$-Cy), 23.1 (s, NH-*C*H$_3$-^{i}Pr), 21.2 (s, N-*C*H$_3$-^{i}Pr). ^{11}B NMR (128 MHz, C_6D_6): δ 2.1 (br, $\Delta\nu_{1/2}$ *ca.* 540 Hz, B).

Reaction of compound 4 with CO

Compound **4** (0.030 g, 0.06 mmol) was dissolved in *ca.* 0.8 mL of C_6D_6 and charged into an NMR tube equipped with a J. Young valve. Then, CO (*ca.* 1 atm) was added through the freeze–pump–thaw procedure. Monitoring of the reaction by ^{1}H NMR revealed that an equilibrium was already reached after 15 min between **4** and the insertion product {^{i}Pr(BC_8H_{14})N}C{N(*p*-Me-C_6H_4)}(N^{i}Pr)(CO)BC_8H_{14} (**14**) with a ratio *ca.* 9 : 1. Partial spectroscopic data for **14**: ^{1}H NMR (500 MHz, C_6D_6): δ 3.74 (sept, 1H, J_{HH} = 6.7 Hz, C*H*-^{i}Pr), 3.31 (m, 1H, C_8H_{14}), 2.93 (sept, 1H, J_{HH} = 6.7 Hz, C*H*-^{i}Pr), 1.97 (s, 3H, *p*-*Me*-C_6H_4), 1.60, 1.53, 0.94, 0.40 (4 × d, 4 × 3H, J_{HH} = 6.7 Hz, 4 × CH_3-^{i}Pr).

Reaction of compound 1 with benzaldehyde

Benzaldehyde (50 μL, 0.50 mmol) was added to a solution of compound **1** (0.018 g, 0.05 mmol) in C_6D_6 (*ca.* 0.8 mL) and the reaction was monitored by ^{1}H NMR in an NMR tube equipped with a J. Young valve. After 4 h at room temperature an equilibrium mixture was reached between the insertion product (Me$_2$N)C(N^{i}Pr)$_2$(PhHCO)BCy_2 (**15**), compound **1** and benzaldehyde, with an approximate ratio of 4 : 9 : 87. Partial spectroscopic data for **15**: ^{1}H NMR (500 MHz, C_6D_6): δ 5.99 (s, 1H, *H*-CPh), 3.98 (sept, 1H, $J_{HH} \approx$ 7 Hz, C*H*-^{i}Pr), 3.35 (sept, 1H, $J_{HH} \approx$ 7 Hz, C*H*-^{i}Pr), 2.29 (s, 6H, N*Me*$_2$), 1.19, 1.10, 0.94, 0.86 (4 × d, 4 × 3H, $J_{HH} \approx$ 7 Hz, 4 × CH_3-^{i}Pr).

Reaction of compound 2 with benzaldehyde

Method A: Benzaldehyde (15 μL, 0.15 mmol) was added to a solution of compound **2** (0.034 g, 0.075 mmol) in C_6D_6 (*ca.* 0.8 mL) and the reaction was monitored by ^{1}H NMR in an NMR tube equipped with a J. Young valve. After 48 h at room temperature an equilibrium was reached between the insertion products {^{i}Pr(H)N}C{N(*p*-^{t}Bu-C_6H_4)}(N^{i}Pr)(PhHCO)BCy_2 (**16a**) and {^{i}Pr(H)N}C(N^{i}Pr){N(*p*-^{t}Bu-C_6H_4)}(PhHCO)BCy_2 (**16b**) and

the reagents, with relative ratios **16a** : **16b** : **2** : benzaldehyde *ca.* 21 : 3 : 17 : 60 at 25 °C. De-insertion is favoured at higher temperatures, and the product ratio changes to 11 : 2 : 28 : 59 upon heating up to 60 °C. Method B: The major insertion product, **16a**, could be isolated as a crystalline solid following this procedure. Benzaldehyde (100 μL, 0.98 mmol) was added to a pentane solution (5 mL) of compound **2** (0.090 g, 0.20 mmol) to form a white suspension which was stirred for 3 h. After this time, pentane was removed under vacuum and *ca.* 0.5 mL of pentane was added to the remaining viscous residue, containing mostly benzaldehyde and a mixture of compounds **16a**, **16b** and **2**. White crystals of **16a** (0.071 g, 63%), which were suitable for an X-ray analysis, were obtained after keeping the latter mixture at −20 °C. Anal. calcd for $C_{36}H_{56}BN_3O$ (**16a**): C, 77.54; H, 10.12; N, 7.54. Found: C, 77.19; H, 9.72; N, 7.29. Spectroscopic data for **16a**: IR (cm^{-1}): ν 3389 (w, N–H). ^{1}H NMR (500 MHz, CD_2Cl_2, 298 K): δ 7.61, 7.39 (AA′MM′X, 2 × 2H, *o*,*m*-Ph), 7.38 (AA′XX′, 2H, *o*,*m*-C_6H_4), 7.31 (AA′MM′X, 1H, *p*-Ph), 7.00 (AA′XX′, 2H, *m*,*o*-C_6H_4), 5.97 (s, 1H, *H*-CPh), 3.87 (sept, J_{HH} = 6.8 Hz, 1H, N-C*H*-^{i}Pr), 3.63 (d, 1H, J_{HH} = 9.4 Hz, N*H*), 3.52 (m, 1H, J_{HH} = 9.4, 6.4 Hz, NH-C*H*-^{i}Pr), 1.7–0.0 (m, 22H, Cy), 1.32 (s, 9H, CH_3-^{t}Bu), 1.27 (d, br, 3H, $J_{HH} \approx 7$ Hz, CH_3-^{i}Pr), 1.10 (d, 3H, J_{HH} = 6.4 Hz, CH_3-^{i}Pr), 1.05 (d, 3H, J_{HH} = 6.8 Hz, CH_3-^{i}Pr), 0.94 (d, 3H, J_{HH} = 6.4 Hz, CH_3-^{i}Pr). ^{13}C{^{1}H} NMR (126 MHz, CD_2Cl_2, 298 K): δ 160.5 (s, *C*N_3), 150.2 (s, *p*-*C*-C_6H_4), 142.0 (s, *ipso*-*C*-Ph), 141–0 (s, *ipso*-*C*-C_6H_4), 128.5 (s, *o*/*m*-*C*-Ph), 127.9 (s, *o*/*m*-*C*-C_6H_4), 127.8 (s, *p*-*C*-Ph), 127.3 (s, *m*/*o*-*C*-Ph), 126.1 (s, *m*/*o*-*C*-C_6H_4), 82.7 (s, H*C*-Ph), 53.8, 50.9 (2 × s, 2 × *C*H-^{i}Pr), 34.8 (s, *C*-^{t}Bu), 32.6 (br, *C*H-Cy), 31.5 (s, *C*H_3-^{t}Bu), 30.7, 29.8, 29.6, 28.4 (4 × br, *C*H_2-Cy), 23.6 (s, 2 × *C*H_3-^{i}Pr), 22.5, 22.1 (2 × s, 2 × *C*H_3-^{i}Pr). ^{11}B NMR (128 MHz, CD_2Cl_2): δ 8.0 (br, $\Delta\nu_{1/2}$ *ca.* 400 Hz, B) ppm. Partial spectroscopic data for **16b**: ^{1}H NMR (500 MHz, C_6D_6): δ 6.36 (s, 1H, *H*-CPh), 4.07 (sept, 1H, $J_{HH} \approx 7$ Hz, N-C*H*-^{i}Pr), 3.89 (d, 1H, J_{HH} = 7.9 Hz, N*H*), 3.14 (m, 1H, NH-C*H*-^{i}Pr).

Reaction of compound 4 with benzaldehyde

Benzaldehyde (60 μL, 0.60 mmol) was added to a solution of compound **4** (0.030 g, 0.06 mmol) in C_6D_6 (*ca.* 0.8 mL) and the reaction was monitored by ^{1}H NMR in an NMR tube equipped with a J. Young valve. A mixture consisting mostly of four compounds: {^{i}Pr(BC_8H_{14})N}C{N(*p*-Me-C_6H_4)}(N^{i}Pr)(PhHCO)BC_8H_{14} (**17**), {^{i}Pr(H)N}C{N(*p*-Me-C_6H_4)}(N^{i}Pr)(PhHCO)BC_8H_{14} (**18**), benzaldehyde and compound **4** was detected after 15 min at room temperature in a ratio *ca.* 6 : 3 : 86 : 5. Partial spectroscopic data for **17**: ^{1}H NMR (500 MHz, C_6D_6): δ 6.35 (s, 1H, *H*-CPh), 4.27 (sept, 1H, J_{HH} = 6.9 Hz, C*H*-^{i}Pr), 3.22 (sept, 1H, J_{HH} = 6.7 Hz, C*H*-^{i}Pr), 2.03 (s, 3H, *p*-*Me*-C_6H_4), 1.31 (d, J_{HH} = 6.9 Hz, CH_3-^{i}Pr), 0.92 (d, J_{HH} = 6.7 Hz, CH_3-^{i}Pr), 0.48 (d, J_{HH} = 6.9 Hz, CH_3-^{i}Pr), 0.40 (d, J_{HH} = 6.7 Hz, CH_3-^{i}Pr). Partial spectroscopic data for **18**: ^{1}H NMR (500 MHz, C_6D_6): δ 6.13 (s, 1H, *H*-CPh), 3.85 (d, 1H, J_{HH} = 8.7 Hz, N*H*), 3.76 (sept, 1H, $J_{HH} \approx 7$ Hz, N-C*H*-^{i}Pr), 3.20 (m, 1H, NH-C*H*-^{i}Pr), 2.00 (s, 3H, *p*-*Me*-C_6H_4), 1.22, 0.78, 0.59, 0.58 (4 × d, 4 × 3H, $J_{HH} \approx 7$ Hz, CH_3-^{i}Pr).

Reaction of compound 2 with CO_2

Compound **2** (0.030 g, 0.07 mmol) was dissolved in *ca.* 0.8 mL of C_6D_6 and charged into an NMR tube equipped with a J. Young valve. Then, CO_2 (*ca.* 1 atm) was added through the freeze–pump–thaw procedure and the reaction was monitored by ^{1}H NMR. After 20 h an equilibrium is reached between the insertion product {^{i}Pr(H)N}C{N(*p*-^{t}Bu-C_6H_4)}(N^{i}Pr)(CO_2)BCy_2 (**19**) and compound **2**, in a ratio *ca.* 9 : 91. Partial spectroscopic data for **19**: ^{1}H NMR (500 MHz, C_6D_6): δ 7.13, 7.01 (AA′XX′, 4H, C_6H_4), 3.88 (sept, 1H, J_{HH} = 6.7 Hz, N-C*H*-^{i}Pr), 3.44 (d, 1H, J_{HH} = 9.2 Hz, N*H*), 2.99 (dsept, 1H, J_{HH} = 9.2, 6.3 Hz, NH-C*H*-^{i}Pr), 1.56 (d, J_{HH} = 6.7 Hz, CH_3-^{i}Pr), 1.15 (s, 9H, CH_3-^{t}Bu), 0.47 (d, J_{HH} = 6.3 Hz, CH_3-^{i}Pr).

General procedure for thermodynamic measurements

In a typical procedure, C_6D_6 solutions (*ca.* 0.8 mL) containing compound **11** or **12** and a known concentration of an internal standard, tetrakis(trimethylsilyl)silane (TKS), were charged into an NMR tube equipped with a J. Young valve. Then, ^{1}H NMR spectra for these solutions were recorded at different temperatures, between 298 and 353 K and the concentrations of **11**/**12** and **4** were calculated by measuring the integrals of their methyne (CH) signals relative to that of the $SiMe_3$ groups of the internal standard (Fig. S2 and S4 in the ESI†).

X-ray crystal determination

X-ray data collection of suitable single crystals was carried out at 100(2) K on a Bruker VENTURE area detector equipped with graphite monochromated Mo-Kα radiation (λ = 0.71073 Å) by applying the ω-scan method. The data reduction was performed with the APEX2[25] software and corrected for absorption using SADABS.[26] Crystal structures were solved by direct methods using the SIR97 program[27] and refined by full-matrix least-squares on F^2 including all reflections using anisotropic displacement parameters by means of the WINGX crystallographic package.[28] All hydrogen atoms were included as fixed contributions riding on attached atoms with isotropic thermal displacement parameters 1.2 times or 1.5 times those of their parent atoms for the organic ligands. In compound **10**, lattice solvent molecules could not be refined owing to their disordered disposition in the voids of the structures, so the electron density at the voids corresponding to one hexane molecule was subtracted from the reflection data by the SQUEEZE procedure as implemented in the PLATON program[29] during the refinement. Details of the structure determination and refinement of compounds **4**, **5**, **8a**, **10**, **11** and **16a** are summarised in Table 5. Crystallographic data (excluding structure factors) for the structures reported in this paper have been deposited with the Cambridge Crystallographic Data Center as supplementary publication numbers CCDC 1554010–1554015.

Theoretical calculations

All DFT computations were carried out using the Gaussian09 package,[30] in which the hybrid method B3LYP was used with the Becke three-parameter exchange functional[31] and the Lee–

Table 5 Crystallographic data and structure refinement details for all compounds

Compound	4	5	8a	10	11	16a
Chem. form.	$C_{30}H_{49}B_2N_3$	$C_{30}H_{50}BN_4$	$C_{37}H_{57}BN_4O$	$C_{55}H_{92}B_2N_4O$	$C_{39}H_{58}B_2N_4$	$C_{36}H_{56}BN_3O$
CCDC	1554013	1554014	1554015	1554010	1554011	1554012
Form. weight	473.34	477.55	584.67	846.94	604.51	557.64
Cryst. system	Triclinic	Monoclinic	Triclinic	Triclinic	Monoclinic	Tetragonal
Space group	$P\bar{1}$	$P2_1/c$	$P\bar{1}$	$P\bar{1}$	$P2_1/n$	$P4_3$
a (Å)	9.858(3)	9.452(2)	10.6730(7)	11.4481(18)	13.906(3)	16.181(4)
b (Å)	10.828(3)	29.608(3)	11.9049(9)	14.078(2)	11.690(3)	16.181(3)
c (Å)	14.100 (4)	10.930(3)	16.1199(11)	16.683(2)	21.696(3)	12.989(3)
α (°)	89.37	90	68.820(2)	69.089(3)	90	90
β (°)	71.462(53)	112.215(4)	85.544(2)	85.835(3)	92.946(4)	90
γ (°)	81.03	90	64.423(2)	75.449(4)	90	90
V (Å^3)	1408.2(6)	2831.7(11)	1715.2(2)	2430.7(6)	3522.3(12)	3400.1(18)
Z	2	4	2	2	4	4
GOF[a]	1.041	1.110	1.042	1.073	1.024	1.078
R_{int}	0.0746	0.1313	0.0853	0.1071	0.0369	0.1418
R_1 [b]/wR^2 [c] [$I > 2\sigma(I)$]	0.0621/0.1278	0.1079/0.2586	0.0521/0.1080	0.0586/0.1420	0.0521/0.1374	0.0463/0.0946
R_1 [b]/wR^2 [c] (all data)	0.1118/0.1461	0.1441/0.2840	0.0924/0.1243	0.1068/0.1629	0.0619/0.1478	0.0707/0.1043

[a] $S = [\sum w(F_o^2 - F_c^2)^2/(N_{obs} - N_{param})]^{1/2}$. [b] $R_1 = \sum||F_o| - |F_c||/\sum|F_o|$. [c] $wR_2 = [\sum w(F_o^2 - F_c^2)^2/\sum wF_o^2]^{1/2}$; $w = 1/[\sigma^2(F_o^2) + (aP)^2 + bP]$ where $P = (\max(F_o^2, 0) + 2F_c^2)/3$.

Yang–Parr correlation functional.[32] An accurate numerical integration grid (99 590) was used for all the calculations *via* the keyword Int = Ultrafine. The light elements (B, N, C and H) were described with the 6-31G* basis.[33] Geometry optimisations used X-ray data of the compounds or related species as the starting point and were performed under no symmetry restrictions. Frequency analyses were performed at all the stationary points to ensure that minimum structures with no imaginary frequencies were achieved. Molecular orbitals and vibrational modes were visualised using the Molekel programme.[34]

Acknowledgements

We gratefully acknowledge financial support from the Ministerio de Economia y Competitividad (MINECO), Spain (grant numbers CTQ2016-77614-R and CTQ2014-51912-REDC). A. R. acknowledges a postdoctoral contract funded by the "Plan Propio de I + D + i" of the Universidad de Castilla-La Mancha, co-funded by the European Social Fund.

Notes and references

1 (*a*) T. Chlupatý and A. Růžička, *Coord. Chem. Rev.*, 2016, **314**, 103–113; (*b*) A. Kurek, P. G. Gordon, S. Karle, A. Devi and S. T. Barry, *Aust. J. Chem.*, 2014, **67**, 989; (*c*) F. T. Edelmann, *Adv. Organomet. Chem.*, 2013, **61**, 55–374; (*d*) S. T. Barry, *Coord. Chem. Rev.*, 2013, **257**, 3192–3201; (*e*) F. T. Edelmann, *Chem. Soc. Rev.*, 2012, **41**, 7657–7672; (*f*) S. Collins, *Coord. Chem. Rev.*, 2011, **255**, 118–138; (*g*) A. A. Trifonov, *Coord. Chem. Rev.*, 2010, **254**, 1327–1347; (*h*) C. Jones, *Coord. Chem. Rev.*, 2010, **254**, 1273–1289; (*i*) F. T. Edelmann, *Chem. Soc. Rev.*, 2009, **38**, 2253–2268; (*j*) M. P. Coles, *Chem. Commun.*, 2009, 3659–3676; (*k*) F. T. Edelmann, *Adv. Organomet. Chem.*, 2008, **57**, 183–352; (*l*) W. E. Piers and D. J. H. Emslie, *Coord. Chem. Rev.*, 2002, **233–234**, 131–155; (*m*) P. J. Bailey and S. Pace, *Coord. Chem. Rev.*, 2001, **214**, 91–141.

2 (*a*) R. Fernández-Galán, J.-A. Navarro, F. Carrillo-Hermosilla, A. Antiñolo, I. López-Solera and E. Villaseñor, *Aust. J. Chem.*, 2014, **67**, 1063; (*b*) D. Elorriaga, F. Carrillo-Hermosilla, A. Antiñolo, I. López-Solera, R. Fernández-Galán and E. Villaseñor, *Dalton Trans.*, 2014, **43**, 17434–17444; (*c*) D. Elorriaga, F. Carrillo-Hermosilla, A. Antiñolo, F. J. Suárez, I. López-Solera, R. Fernández-Galán and E. Villaseñor, *Dalton Trans.*, 2013, **42**, 8223–8230; (*d*) D. Elorriaga, F. Carrillo-Hermosilla, A. Antiñolo, I. López-Solera, R. Fernández-Galán and E. Villaseñor, *Chem. Commun.*, 2013, **49**, 8701–8703; (*e*) D. Elorriaga, F. Carrillo-Hermosilla, A. Antiñolo, I. López-Solera, R. Fernández-Galán, A. Serrano and E. Villaseñor, *Eur. J. Inorg. Chem.*, 2013, 2940–2946; (*f*) R. Fernández-Galán, A. Antiñolo, F. Carrillo-Hermosilla, I. López-Solera, A. Otero, A. Serrano-Laguna and E. Villaseñor, *Organometallics*, 2012, **31**, 8360–8369; (*g*) R. Fernández-Galán, A. Antiñolo, F. Carrillo-Hermosilla, I. López-Solera, A. Otero, A. Serrano-Laguna and E. Villaseñor, *J. Organomet. Chem.*, 2012, **711**, 35–42; (*h*) D. Elorriaga, F. Carrillo-Hermosilla, A. Antiñolo, I. López-Solera, B. Menot, R. Fernández-Galán, E. Villaseñor and A. Otero, *Organometallics*, 2012, **31**, 1840–1848.

3 (*a*) C. Alonso-Moreno, F. Carrillo-Hermosilla, A. Garcés, A. Otero, I. López-Solera, A. M. Rodríguez and A. Antiñolo, *Organometallics*, 2010, **29**, 2789–2795; (*b*) J. Francos, P. J. González-Liste, L. Menéndez-Rodríguez, P. Crochet, V. Cadierno, J. Borge, A. Antiñolo, R. Fernández-Galán and F. Carrillo-Hermosilla, *Eur. J. Inorg. Chem.*, 2016, **2016**, 393–402; (*c*) L. Menéndez-Rodríguez, E. Tomás-Mendivil,

J. Francos, P. Crochet, V. Cadierno, A. Antiñolo, R. Fernández-Galán and F. Carrillo-Hermosilla, *Organometallics*, 2015, **34**, 2796–2809.

4 M. De Tullio, A. Hernán-Gómez, Z. Livingstone, W. Clegg, A. R. Kennedy, R. W. Harrington, A. Antinolo, A. Martínez, F. Carrillo-Hermosilla and E. Hevia, *Chem. – Eur. J.*, 2016, **22**, 17646–17656.

5 (*a*) D. Nieto, S. Bruña, A. M. González-Vadillo, J. Perles, F. Carrillo-Hermosilla, A. Antiñolo, J. M. Padrón, G. B. Plata and I. Cuadrado, *Organometallics*, 2015, **34**, 5407–5417; (*b*) J. Romero-Fernández, F. Carrillo-Hermosilla, A. Antiñolo, C. Alonso-Moreno, A. M. Rodríguez, I. López-Solera and A. Otero, *Dalton Trans.*, 2010, **39**, 6419–6425; (*c*) A. Antiñolo, F. Carrillo-Hermosilla, R. Fernández-Galán, J. Martínez-Ferrer, C. Alonso-Moreno, I. Bravo, S. Moreno-Blázquez, M. Salgado, E. Villaseñor and J. Albaladejo, *Dalton Trans.*, 2016, **45**, 10717–10729.

6 A. Antiñolo, F. Carrillo-Hermosilla, R. Fernández-Galán, M. P. Montero-Rama, A. Ramos, E. Villaseñor, R. S. Rojas and A. Rodríguez-Diéguez, *Dalton Trans.*, 2016, **45**, 15350–15363.

7 (*a*) R. Jefferson, M. F. Lappert, B. Prokai and B. P. Tilley, *J. Chem. Soc. A*, 1966, 1584–1590; (*b*) D. J. Brauer, S. Buchheim-Spiegel, H. Bürger, R. Gielen, G. Pawelke and J. Rothe, *Organometallics*, 1997, **16**, 5321–5330; (*c*) G. A. Pierce, N. D. Coombs, D. J. Willock, J. K. Day, A. Stasch and S. Aldridge, *Dalton Trans.*, 2007, 4405–4412; (*d*) M. Findlater, N. J. Hill and A. H. Cowley, *Dalton Trans.*, 2008, 4419–4423; (*e*) H. Braunschweig, R. D. Dewhurst, K. Schwab and K. Wagner, *Acta Crystallogr., Sect. E: Struct. Rep. Online*, 2010, **66**, o610; (*f*) C. Jones, D. P. Mills, A. Stasch and W. D. Woodul, *Main Group Chem.*, 2010, **9**, 23–30.

8 M. A. Dureen and D. W. Stephan, *J. Am. Chem. Soc.*, 2010, **132**, 13559–13568.

9 B. M. Mikhailov, V. A. Dorokhov and L. I. Lavrinovich, *Russ. Chem. Bull.*, 1978, **27**, 2304–2310.

10 V. A. Dorokhov, L. I. Lavrinovich and B. M. Mikhailov, *Dokl. Akad. Nauk SSSR*, 1979, **245**, 121–125.

11 V. A. Dorokhov, I. P. Yakovlev and B. M. Mikhailov, *Russ. Chem. Bull.*, 1980, **29**, 485–491.

12 R. Boese, R. Koester and M. Yalpani, *Z. Naturforsch., B: Chem. Sci.*, 1994, **49**, 1453–1458.

13 M. F. Lappert, P. P. Power, A. R. Sanger and R. C. Srivastava, *Metal and metalloid amides: syntheses, structures, and physical and chemical properties*, ed. E. Horwood, 1980.

14 L. Yang, X. Ren, H. Wang, N. Zhang and S. Hong, *Res. Chem. Intermed.*, 2011, **38**, 113–133.

15 (*a*) A. J. P. Cardenas, Y. Hasegawa, G. Kehr, T. H. Warren and G. Erker, *Coord. Chem. Rev.*, 2016, **306**, 468–482; (*b*) O. Ekkert, G. G. Miera, T. Wiegand, H. Eckert, B. Schirmer, J. L. Petersen, C. G. Daniliuc, R. Fröhlich, S. Grimme, G. Kehr and G. Erker, *Chem. Sci.*, 2013, **4**, 2657.

16 A. C. McQuilken, Q. M. Dao, A. J. P. Cardenas, J. A. Bertke, S. Grimme and T. H. Warren, *Angew. Chem., Int. Ed.*, 2016, **55**, 14335–14339.

17 A. R. Cabrera, R. S. Rojas, M. Valderrama, P. Pluss, H. Berke, C. G. Daniliuc, G. Kehr and G. Erker, *Dalton Trans.*, 2015, **44**, 19606–19614.

18 C. M. Momming, E. Otten, G. Kehr, R. Frohlich, S. Grimme, D. W. Stephan and G. Erker, *Angew. Chem., Int. Ed.*, 2009, **48**, 6643–6646.

19 R. Taylor and O. Kennard, *J. Am. Chem. Soc.*, 1982, **104**, 5063–5070.

20 S. Fukumoto, T. Nakashima and T. Kawai, *Angew. Chem., Int. Ed.*, 2011, **50**, 1565–1568.

21 (*a*) F. Sánchez-Viesca and M. Berros, *Heterocycles*, 2002, **57**, 1869–1879; (*b*) A. V. Afonin, D. V. Pavlov, A. I. Albanov, O. A. Tarasova and N. A. Nedolya, *Magn. Reson. Chem.*, 2013, **51**, 414–423.

22 S. Mummadi, D. K. Unruh, J. Zhao, S. Li and C. Krempner, *J. Am. Chem. Soc.*, 2016, **138**, 3286–3289.

23 B. R. Barnett, C. E. Moore, A. L. Rheingold and J. S. Figueroa, *Chem. Commun.*, 2015, **51**, 541–544.

24 (*a*) C. M. Momming, G. Kehr, B. Wibbeling, R. Frohlich and G. Erker, *Dalton Trans.*, 2010, **39**, 7556–7564; (*b*) L. M. Elmer, G. Kehr, C. G. Daniliuc, M. Siedow, H. Eckert, M. Tesch, A. Studer, K. Williams, T. H. Warren and G. Erker, *Chem. – Eur. J.*, 2017, **23**, 6056–6068.

25 Bruker Apex2, Bruker AXS Inc., Madison, Wisconsin, USA, 2004.

26 G. M. Sheldrick, SADABS, Program for Empirical Adsorption Correction, Institute for Inorganic Chemistry, University of Gottingen, Germany, 1996.

27 A. Altomare, M. C. Burla, M. Camalli, G. L. Cascarano, C. Giacovazzo, A. Guagliardi, A. G. G. Moliterni, G. Polidori and R. Spagna, *J. Appl. Crystallogr.*, 1999, **32**, 115–119.

28 G. M. Sheldrick, *SHELX-2014, Program for Crystal Structure Refinement*, University of Göttingen, Göttingen, Germany, 2014.

29 A. L. Spek, *J. Appl. Crystallogr.*, 2003, **36**, 7–13.

30 M. J. Frisch, G. W. Trucks, H. B. Schlegel, G. E. Scuseria, M. A. Robb, J. R. Cheeseman, G. Scalmani, V. Barone, B. Mennucci, G. A. Petersson, H. Nakatsuji, M. Caricato, X. Li, H. P. Hratchian, A. F. Izmaylov, J. Bloino, G. Zheng, J. L. Sonnenberg, M. Hada, M. Ehara, K. Toyota, R. Fukuda, J. Hasegawa, M. Ishida, T. Nakajima, Y. Honda, O. Kitao, H. Nakai, T. Vreven, J. A. Montgomery, J. E. Peralta, F. Ogliaro, M. Bearpark, J. J. Heyd, E. Brothers, K. N. Kudin, V. N. Staroverov, R. Kobayashi, J. Normand, K. Raghavachari, A. Rendell, J. C. Burant, S. S. Iyengar, J. Tomasi, M. Cossi, N. Rega, J. M. Millam, M. Klene, J. E. Knox, J. B. Cross, V. Bakken, C. Adamo, J. Jaramillo, R. Gomperts, R. E. Stratmann, O. Yazyev, A. J. Austin, R. Cammi, C. Pomelli, J. W. Ochterski, R. L. Martin, K. Morokuma, V. G. Zakrzewski, G. A. Voth, P. Salvador, J. J. Dannenberg, S. Dapprich, A. D. Daniels, O. Farkas, J. B. Foresman, J. V. Ortiz, J. Cioslowski and D. J. Fox, *Gaussian 09, Revision B.01*, Wallingford CT, 2009.

31 A. D. Becke, *J. Chem. Phys.*, 1993, **98**, 5648–5652.
32 C. Lee, W. Yang and R. G. Parr, *Phys. Rev. B: Condens. Matter*, 1988, **37**, 785–789.
33 (*a*) P. C. Hariharan and J. A. Pople, *Theor. Chim. Acta*, 1973, **28**, 213–222; (*b*) G. A. Petersson, A. Bennett, T. G. Tensfeldt, M. A. Al-Laham, W. A. Shirley and J. Mantzaris, *J. Chem. Phys.*, 1988, **89**, 2193–2218; (*c*) G. A. Petersson and M. A. Al-Laham, *J. Chem. Phys.*, 1991, **94**, 6081–6090.
34 S. Portmann and H. P. Lüthi, *Chimia*, 2000, **54**, 766–770.